Dedicated to the memory of our colleague prof. A.A. Pasynskii

Salts and Complexes Containing the Decachloro-*closo*-Decaborate Anion

V. V. Avdeeva[a], *, E. A. Malinina[a], K. Yu. Zhizhin[a], and N. T. Kuznetsov[a]

[a] *Kurnakov Institute of General and Inorganic Chemistry, Russian Academy of Sciences, Moscow, 119991 Russia*
e-mail: avdeeva.varvara@mail.ru

Abstract—This work describes the currently known cationic-anionic and complex metal compounds containing the decachloro-*closo*-decaborate anion $[B_{10}Cl_{10}]^{2-}$. The influence of the nature of the cation, solvent, metal and/or organic ligands on the composition and structure of the reaction products is discussed. Salts and complexes containing alkali metal cations, organic cations, and cationic complexes of metals Ag(I), Cu(II), Fe(II), Co(II), Ni(II), and Mn(II) with the decachloro-*closo*-decaborate anion as a counterion are described. The first examples of silver(I) complexes with the coordinated $[B_{10}Cl_{10}]^{2-}$ anion are described. The ability of the perchlorinated *closo*-decaborate anion to participate in additional non-bonded interactions B−Cl...X (X = C, N, O) with alkali metal cations, organic cations, organic ligands, and solvent molecules is discussed; these interactions can be identified by ^{35}Cl NQR spectroscopy and X-ray diffraction. A number of new compounds based on perchlorinated boron clusters $[B_{10}Hal_9R]^-$ containing nine halogen atoms and a functional group R are discussed.

INTRODUCTION

Boron cluster anions include compounds of the general formula $[B_nH_n]^{2-}$ ($n = 6-12$) [1–3], which are closed bulk polyhedra built of boron atoms. In turn, each boron atom is bonded to an exo-polyhedral hydrogen atom. Polyhedral boron anions $[B_nH_n]^{2-}$ ($n = 6-12$) posess three-dimensional aromaticity and tend to participate in the reactions of substitution of terminal hydrogen atoms with the retention of the boron cage, forming substituted derivatives with the number of substituents from 1 to n. Interest in this class of anions is due to wide possibilities of varying their electronic structure as well as geometric and physical characteristics, which makes it possible to obtain compounds with desired properties. The specific features of the chemical behavior of boron cluster anions and their derivatives, the thermal and kinetic stability of compounds based on them are primarily associated with the structural features of these objects [4–6].

The most interesting areas of practical application of compounds containing boron cluster anions and their substituted derivatives have traditionally been considered the areas of science associated with the high-energy content of these compounds. The ability

of the boron atom to absorb thermal neutrons discovered later significantly expanded the application field of boron-containing compounds and served as the basis for using the latter as precursors for creating strong heat-resistant polymer neutron-protective coatings with good adhesion to various materials, neutron-protective tissues and materials [7–9], and contrast agents for MRI diagnostics [10]. Metal complexes with $[B_nH_n]^{2-}$ anions have found wide application as extractants of heavy metals, precursors of metal borides of complex composition, coordination polymers, compounds with high energy intensity, etc. [11–14].

Some problems in the chemistry of boron cluster anions, their structure, and the ability to replace exo-polyhedral hydrogen atoms with various functional groups while retaining the boron cage are described in reviews [15–25]. These studies describe the synthesis, structure, and properties of metal salts and complexes containing 10-, 11- and 12-vertex boron clusters $[B_nH_n]^{2-}$ being compounds with higher synthetic availability compared to other boron clusters $[B_nH_n]^{2-}$. Until recently, the chemical behavior of perhalogenated boron cluster anions in complexation reactions
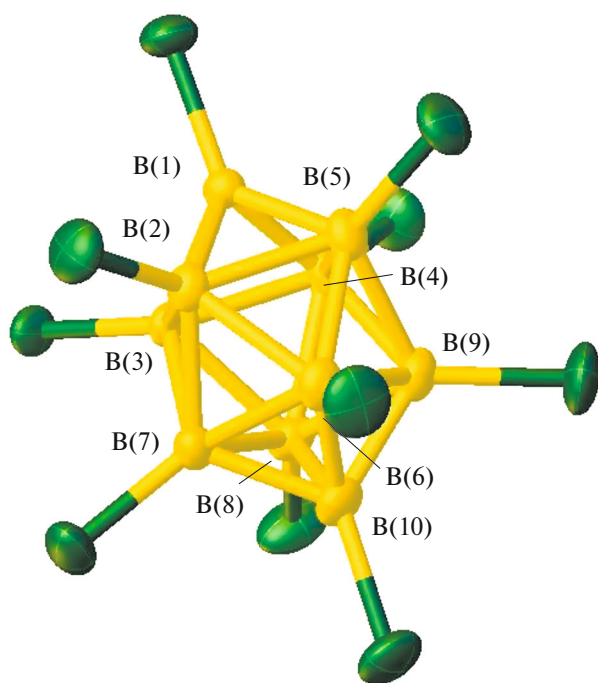
Fig. 1. Structure of the $[B_{10}Cl_{10}]^{2-}$ anion.

was practically not studied, and the information available in the literature was scattered.

This review summarizes the information on salts and complexes containing the decachloro-*closo*-decaborate anion $[B_{10}Cl_{10}]^{2-}$, discusses the redox processes occurring in reaction solutions, the preparation conditions, and the structural features of the final compounds.

PREPARATION AND IDENTIFICATION OF COMPOUNDS WITH DECACHLORO-*closo*-DECABORATE ANION

Simple salts of the decachloro-*closo*-decaborate anion are obtained by chlorination of the salts of the unsubstituted anion $[B_{10}H_{10}]^{2-}$ with chlorinating agents such as chlorine gas or $SOCl_2$. In this case, a number of products with various degrees of substitution $[B_{10}H_{10-x}Cl_x]^{2-}$ ($x = 1-10$) can be formed, which can be separated chromatographically or using electrophoresis [26–28]. Generalization of the structure of compounds $[B_{10}H_{10-x}Cl_x]^{2-}$ ($x = 1-9$) are beyond the scope of this review. We only note that a number of compounds with a partially chlorinated *closo*-decaborate anion were studied by X-ray diffraction, for example $[(C_5H_5N)_2CH_2][2-B_{10}H_9Cl]$ [29], $(Me_4N)[1,6,8-B_{10}H_7Cl_3]$ [30], $3-CH_3-2,8-[NMe_2(CH_2Cl)]_2-7-Cl-B_{10}H_6$ [31], and $(Ph_3(NaphCH_2)P)_2[B_{10}H_8Cl_2]$ [32].

Compounds containing the $[B_{10}Cl_{10}]^{2-}$ anion can be identified using IR, NMR, and Raman spectrosco-

pies [33–35]. Geometrically, the perchlorinated anion $[B_{10}Cl_{10}]^{2-}$ is a square Archimedean antiprism (Fig. 1). In the IR spectrum of the compounds, the bands of stretching vibrations ν(B−Cl) are observed in the region of 1150 and 1000 cm^{-1}, as well as a band at about 850 cm^{-1} corresponding to the B−B stretching vibrations of the boron cage. The Raman spectrum clearly shows an intense band at 310 cm^{-1}, which corresponds to the stretching vibrations of B_{10}−Cl. In the ^{11}B NMR spectrum of solutions of salts with the perchlorinated anion, two signals are observed with an integrated intensity ratio of 1 : 4, which corresponds to the presence of two types of boron atoms in the polyhedron, apical and equatorial ones. In contrast to the spectra of the unsubstituted anion, in the absence of broadband suppression of the B−H spin−spin interaction, the signals are not split into doublets, remaining singlet. The authors [36] present the data of photoelectron spectroscopy and voltammetry of $[B_nCl_n]^{2-}$ clusters ($n = 10, 11, 12$) and conclude that the B_{10} and B_{12} clusters are more stable as compared with the B_{11} boron cluster.

The NQR spectroscopy method can be used to identify compounds with the decachloro-*closo*-decaborate anion. This method is useful due to the high sensitivity of the NQR spectral parameters to the features of the electronic distribution, geometric structure, and stereochemistry of compounds and has been used for other objects as an effective method for studying the crystal chemistry of compounds [37]. The results of ^{35}Cl NQR spectroscopy studies carried out for a number of compounds containing the $[B_{10}Cl_{10}]^{2-}$ anion showed the possibility of this method to determine from the entire set of interatomic contacts determined by X-ray diffraction analysis those caused by secondary attraction interactions [38].

The $[B_{10}Cl_{10}]^{2-}$ dianion forms cationic-anionic compounds with various cations, including alkali metal cations, organic and complex cations. Based on the data of X-ray diffraction, these compounds, as a rule, form a branched network of secondary interactions with the participation of the B−Cl groups of the boron cluster. The hypothetical ^{35}Cl NQR spectrum of a "free" boron cluster that does not participate in any interactions should represent two signals with an intensity ratio of 1 : 4, which corresponds to the presence of two types of chlorine atoms that are linked to the apical and equatorial boron atoms of the polyhedron. The participation of chlorine atoms in secondary interactions leads to the removal of equivalence, which leads to the splitting of the two components.

The paper presents the results of X-ray diffraction studies of compounds containing the *closo*-decaborate anion $[B_{10}Cl_{10}]^{2-}$, and for a number of compounds we show the data of ^{35}Cl NQR spectroscopy, which makes it possible to discuss the nature of secondary interactions in which the boron cluster participates.

CHEMICAL BEHAVIOR OF DECACHLORO-*closo*-DECABORATE ANION IN REDOX REACTIONS

It is known that the *closo*-decaborate anion $[B_{10}Cl_{10}]^{2-}$ undergoes reversible electrochemical oxidation ($E_{1/2} = 1.01$ V) with the formation of the *hyper-closo*-$[B_{10}Cl_{10}]^{-}$ radical, which imparts a deep violet color to the reaction solution [39, 40]. The $[B_{10}Cl_{10}]^{-}$ radical anion can also be obtained by chemical oxidation of the $[B_{10}Cl_{10}]^{2-}$ anion with oxidizing agents such as cerium(IV) [41] or thallium(III) [39]. Another method of preparation was described by the authors [42]: the radical anion is formed by treating salts of the $[B_{10}Cl_{10}]^{2-}$ anion with thionyl chloride in dichloroethane or by controlled dehydrogenation of $H_2[B_{10}Cl_{10}]\cdot 7.5H_2O$ at $100-160°C$.

The study of the chemical behavior of the decachloro-*closo*-decaborate anion in the iron(III) and cobalt(III) complexation accompanied by redox transformations showed that the $[B_{10}Cl_{10}]^{2-}$ anion does not stabilize the indicated oxidation states of metals. When $(Et_3NH)_2[B_{10}Cl_{10}]$ was allowed to react with iron(III) sulfate or chloride, iron(II) complexes with the composition $[Fe^{II}L_3][B_{10}Cl_{10}]$ are formed, with the yield of complexes not exceeding 65% [43].

$$Fe^{3+} + [B_{10}Cl_{10}]^{2-} + 3L \xrightarrow{CH_3CN} [Fe^{II}L_3][B_{10}Cl_{10}]$$
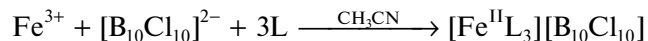
L = 2,2'-bipyridine (Bipy)
or 1,10-phenanthroline (Phen)

The boron cluster anion behaves similarly in complexation in the presence of cobalt(III). The introduction of a salt of the $[B_{10}Cl_{10}]^{2-}$ cluster anion into the reaction solution containing the cobalt(III) complex in situ led to the formation of the corresponding cobalt(II) $[Co(Phen)_3][B_{10}Cl_{10}]$ [44], the structure of which will be described below.

$$Co^{II}Cl_2 + 3Phen + (NH_4)_2Ce^{IV}(NO_3)_6 \xrightarrow{CH_3CN/H_2O} [Co^{III}(Phen)_3]^{3+} \text{ (in situ),}$$

$$[Co^{III}(Phen)_3]^{3+} \text{ (in situ)} + [B_{10}Cl_{10}]^{2-} \xrightarrow{CH_3CN/H_2O} [Co(Phen)_3][B_{10}Cl_{10}].$$
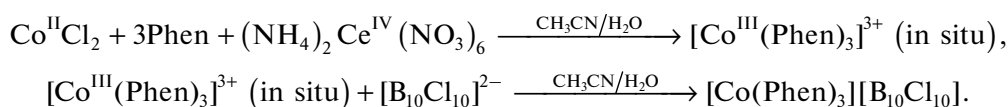
CATIONIC-ANIONIC COMPOUNDS WITH DECACHLORO-*closo*-DECABORATE ANION

Salts with Alkali Metal Cations

Solvates $K_2[B_{10}Cl_{10}]\cdot 3H_2O$ and $K_2[B_{10}Cl_{10}]\cdot DMF\cdot 2H_2O$, the structures of which are shown in Fig. 2, are formed in the course of recrystallization of $K_2[B_{10}Cl_{10}]$ in water or *N,N*-dimethylformamide, respectively. In the IR spectra of the salts of the perchlorinated anion, two intense broad bands $\nu(BCl)$ with maxima at about 1150 and 1010 cm^{-1} are observed, corresponding to the stretching vibrations of the apical and equatorial B−Cl groups, respectively. According to X-ray diffraction data, in compound $K_2[B_{10}Cl_{10}]\cdot 3H_2O$, a large number of contacts of chlorine atoms with the potassium atoms and water molecules are determined. Trihydrate $K_2[B_{10}Cl_{10}]\cdot 3H_2O$ was studied by ^{35}Cl NQR spectroscopy. Based on the data obtained, it is shown (Fig. 2b) that hydrogen and potassium atoms contribute to the electric field gradient on chlorine atoms [45]. Thus, in compound $K_2[B_{10}Cl_{10}]\cdot 3H_2O$, based on the X-ray diffraction and ^{35}Cl NQR spectroscopy data, one can assume the presence of Cl...H and Cl...O interactions (the shortest distance is 2.277 and 3.062 Å, respectively). Note that in the IR spectrum of compounds the presence of secondary interactions is not reflected by any changes, while for salts with unsubstituted $[B_nH_n]^{2-}$ anions, changes in the IR spectra are clearly manifested in the region of stretching vibrations $\nu(BH)$.

Recrystallization of salt $Cs_2[B_{10}Cl_{10}]$ from an aqueous solution yielded two solvates differing in the number of water molecules, namely $Cs_2[B_{10}Cl_{10}]\cdot 2H_2O$ and $Cs_2[B_{10}Cl_{10}]\cdot H_2O$ [40]. According to the X-ray diffraction data (Fig. 3a), $Cs_2[B_{10}Cl_{10}]\cdot 2H_2O$ dihydrate contains one cluster anion per unit cell. Among the distances determined by X-ray diffraction, three (O−H...Cl) contacts can be distinguished, the values of which are less than the van der Waals distances (2.863, 2.536, and 2.570 Å). The contribution of cesium atoms to the gradient on the chlorine atom is insignificant due to the very high coordination numbers of the latter (from 9 to 11). The authors [46] note that the unit cell of $Cs_2[B_{10}Cl_{10}]\cdot 2H_2O$ dihydrate contains cesium atoms disordered over two positions with approximately equal occupancies.

The ^{35}Cl NQR spectrum of dihydrate $Cs_2[B_{10}Cl_{10}]\cdot 2H_2O$ is shown in Fig. 3b. It follows from the data presented that the nature of the spectrum of the compound is closest to the theoretically possible spectrum of the free $[B_{10}Cl_{10}]^{2-}$ anion, which is not bonded to other components of the structure.

The structure of the monosolvate $Cs_2[B_{10}Cl_{10}]\cdot H_2O$ is more complex (Fig. 4). The cell contains four independent decachloro-*closo*-decaborate anions. The structure contains a large number of specific B−Cl...H interactions with the shortest distance 2.518 Å. Based on X-ray diffraction data, the authors suggest the presence of non-bonded B−Cl...H interactions with the participation of chlorine atoms [46].
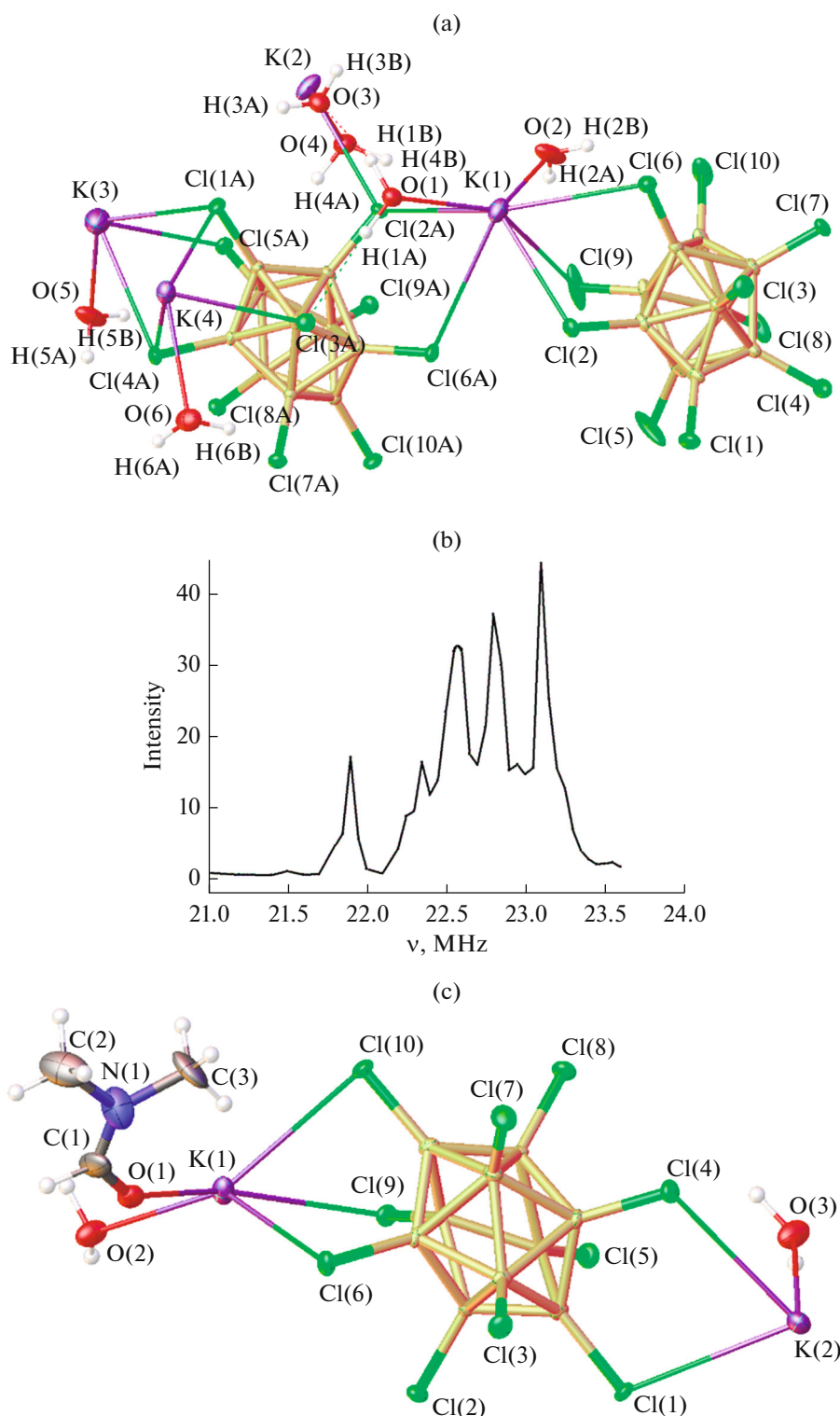
(a)

(b)

(c)

Fig. 2. (a) Fragment of the structure and (b) ^{35}Cl NQR spectrum of solvate $K_2[B_{10}Cl_{10}]\cdot3H_2O$; (c) fragment of the structure of $K_2[B_{10}Cl_{10}]\cdot DMF\cdot2H_2O$.

Salts with Organic Cations

Salts with organic cations were obtained by adding the corresponding chlorides to the salts with alkali metal cations. For a number of salts of the decachloro- *closo*-decaborate anion with organic cations, ^{35}Cl NQR spectra were studied and X-ray diffraction was performed. It was found that compound $(Ph_4P)_2[B_{10}Cl_{10}]$ crystallizes as associate $(Ph_4P)_2$-
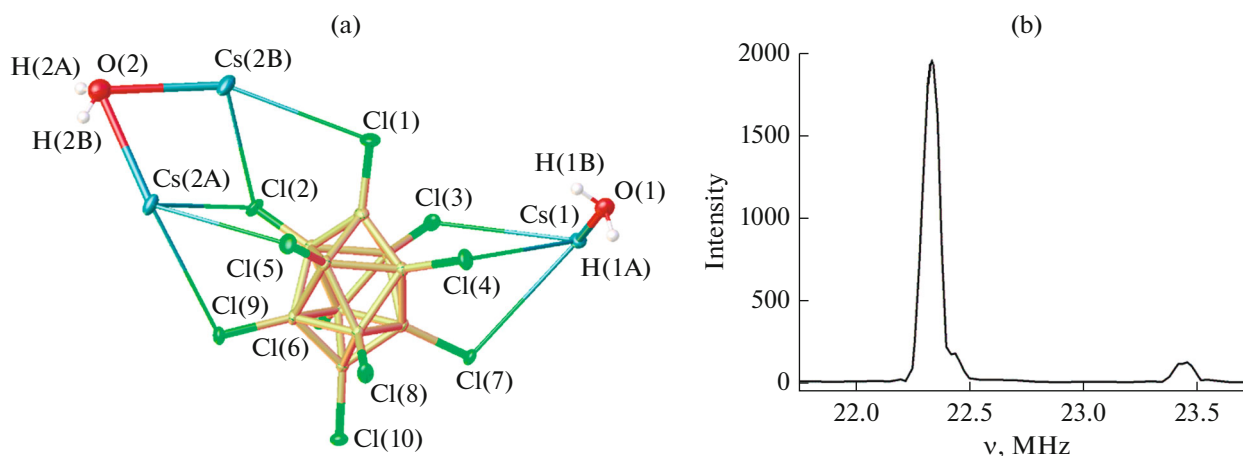
Fig. 3. (a) Fragment of the structure and (b) [35]Cl NQR spectrum of salt $Cs_2[B_{10}Cl_{10}]\cdot2H_2O$.

$[B_{10}Cl_{10}]\cdot CH_3CN$ [47]; its structure is shown in Fig. 5. According to X-ray diffraction data, in the structure of $(Ph_4P)_2[B_{10}Cl_{10}]\cdot CH_3CN$, in addition to hydrogen bonds detected by X-ray diffraction, a large number of the Cl...C and Cl...N contacts can be distinguished, in which the distance between atoms is shorter than the sum of van der Waals radii of interacting atoms. In addition, the compound contains $\pi-\pi$ stacking interactions between the aromatic systems of the boron cluster of the anion and the phenyl rings of the cation.

From the pattern of the [35]Cl NQR spectrum (Fig. 5c), it can be concluded that the compound contains at least four B−Cl...H bonds and one shortened B−Cl...C contact, which should be attributed to the structural manifestation of the $\pi-\pi$ stacking interaction. The shortest Cl...C distance is 3.351 Å [47].

In [47], the structure of salt $(Et_3NH)_2[B_{10}Cl_{10}]$ was analyzed based on [35]Cl NQR spectroscopy and X-ray diffraction. The [35]Cl NQR spectrum of the compound is strongly split (Fig. 6a), which can be explained by the presence of long-range contacts with the CH and NH groups of the organic cation. The multiplicity of the spectrum exceeds ten, which indicates the existence of several crystallographically nonequivalent boron clusters in the crystal lattice of the compound, and at least twelve Cl atoms are involved in secondary interactions. In the [35]Cl NQR spectrum of salt $(Et_3NH)_2[B_{10}Cl_{10}]$ recorded at 77 K, there is no frequency shift upon heating the sample from 19 to 77 K (Fig. 6b) [47].

The presence of the nonequivalent $[B_{10}Cl_{10}]^{2-}$ anions in the crystal cell of salt $(Et_3NH)_2[B_{10}Cl_{10}]$ was confirmed by X-ray powder diffraction (Fig. 6c). According to the data obtained, the unit cell parameters are $a = 26.3857$, $b = 10.3570$, $c = 30.3518$ Å, $\beta = 123.43°$, $V = 6406.5$ Å[3], space group $P2_1/c$ ($R_{Bragg} = 0.068$, $R_{wp} = 2.50$), which corresponds to the presence of four crystallographically nonequivalent cations and two crystallographically independent anions in the cell. In this compound, one can assume the presence of not only the C−H...Cl interactions but also the N−H...Cl contacts, which are responsible for the strong splitting of the [35]Cl NQR spectrum.

The synthesis and structures of $[C_nMim]_2[B_{10}Cl_{10}]$ ($[C_nMim]^+$ = (1-alkyl-3-methylimidazolium; n = 2, 4, 6, 8, 10, 12, 14, 16, 18) were reported [48]; the thermal properties of the compounds were studied. It was found that the salts have low melting points, and the possibility of obtaining ionic liquids based on the obtained compounds was shown.

Cationic-Anionic Compounds with Complex Cations

Cationic metal complexes with organic ligands or solvent molecules present in the reaction solution can act as cations in compounds with the perchlorinated boron cluster. In this case, boron cluster anions are located in the outer sphere of the complexes, participating in the formation of non-bonded interactions.

Iron(II) complexes. In the reactions of iron(II) complexation with the $[B_{10}Cl_{10}]^{2-}$ anion in the presence of organic ligands, it was found that regardless of the solvent used and the ratio of reagents (Fe : L = 1 : 1, 1 : 2, 1 : 3), tris-chelate complexes $[FeL_3][B_{10}Cl_{10}]$ (L = Bipy, Phen) [43] are formed. The formation of these compounds is explained by the high stability of the tris-chelate cationic complexes $[FeL_3]^{2+}$ in the reaction solution.

$$Fe^{2+} + 3L \rightarrow [FeL_3]^{2+},$$

$$[FeL_3]^{2+} + [B_{10}Cl_{10}]^{2-} \rightarrow [FeL_3][B_{10}Cl_{10}].$$
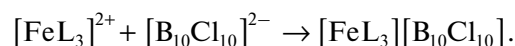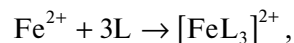
Tris-chelate complexes of the general formula $[FeL_3][B_{10}Cl_{10}]$ are isolated from reaction solutions in the form of solvates with solvent molecules contained in the reaction mixture (H_2O, CH_3CN, and DMF). A
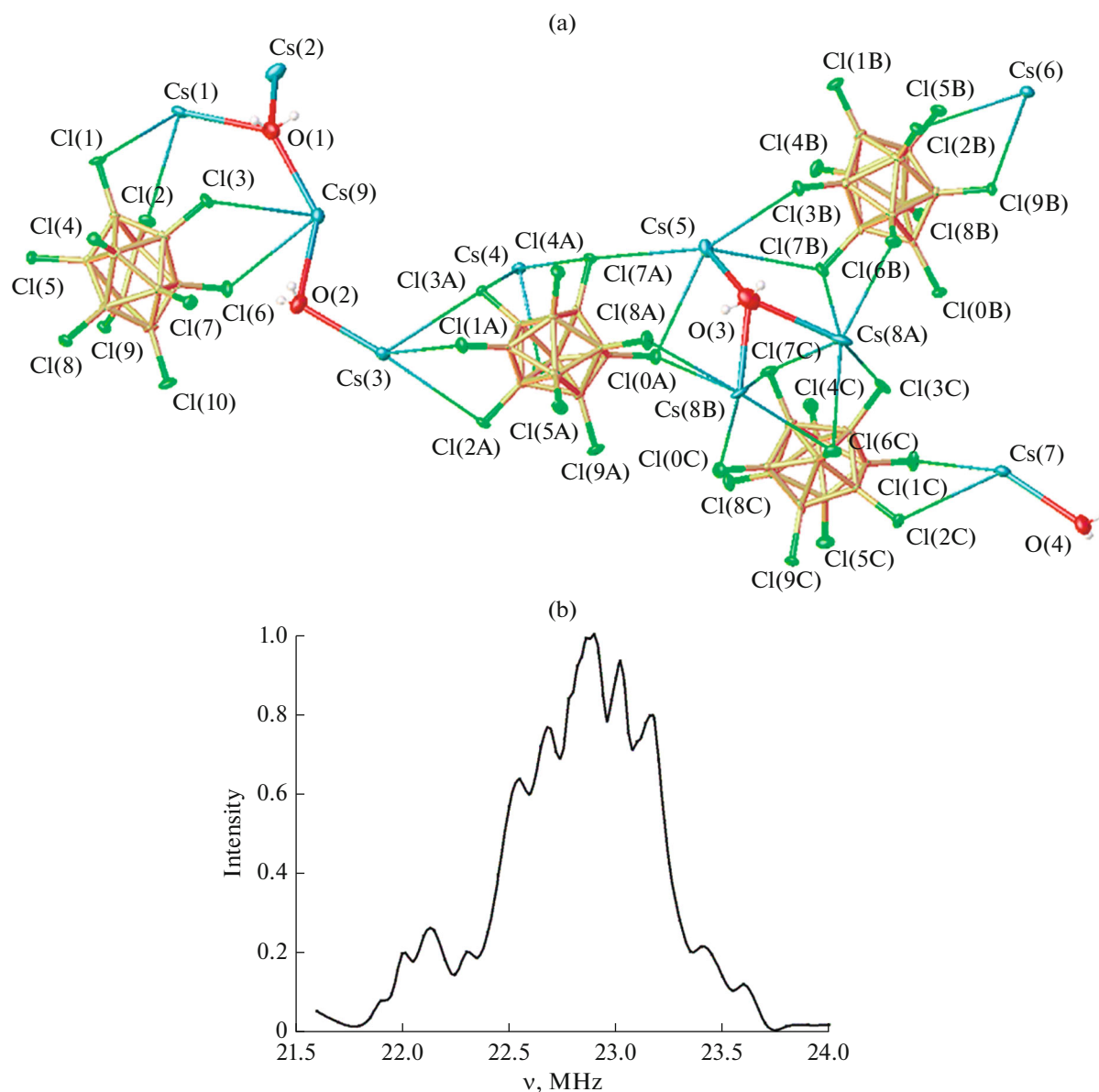
(a)

(b)

Fig. 4. (a) Fragment of the structure and (b) ^{35}Cl NQR spectrum at 77 K of salt $Cs_2[B_{10}Cl_{10}] \cdot H_2O$.

number of solvates were characterized by X-ray diffraction; their structures are shown in Fig. 7. According to the data obtained, the compounds are built of cationic complexes $[FeL_3]^{2+}$, boron cluster anions, and solvent molecules. Complex $[Fe(Bipy)_3][B_{10}Cl_{10}] \cdot 2CH_3CN \cdot H_2O$ (Fig. 7b) contains three crystallographically independent cationic iron(II) complexes and three boron cluster anions; in complex $[Fe(Phen)_3][B_{10}Cl_{10}] \cdot 0.88CH_3CN \cdot 0.12H_2O$ (Fig. 7c), one of the three coordinated Phen molecules is disordered over three positions. Boron cluster anions in all compounds form the outer sphere of the complexes. An increase in the excess of the ligand with respect to the metal leads to the formation of cocrystal $[Fe(Bipy)_3][B_{10}Cl_{10}] \cdot 2Bipy \cdot CH_3CN$ (Fig. 7d), in

which the Bipy molecule is incorporated into the crystal structure.

The synthesis and structure of iron complexes $[Cat][B_{10}Cl_{10}]$, where $[Cat]^{2+}$ is $[Fe(HTrz)_3]^{2+}$ (HTrz is 1,2,4-triazole), $[Fe(NH_2Trz)_3]^{2+}$ (NH$_2$Trz is 4-amino-1,2,4-triazole), and $[Fe(HC(Pz)_3)_2]^{2+}$ (HC(Pz)$_3$ is tris(pyrazol-1-yl)methane) were reported [49]; their IR, EXAFS, and EAS spectra as well as static magnetic susceptibility in the range 78–500 K were studied. It was shown that complexes with $[Cat] = [Fe(Htrz)_3]^{2+}$ and $[Fe(NH_2Trz)_3]^{2+}$ in the considered temperature range remain in the high-spin state, while in the spectrum of low-spin complex $[Fe(HC(Pz)_3)_2][B_{10}Cl_{10}]$, an incomplete spin transi-
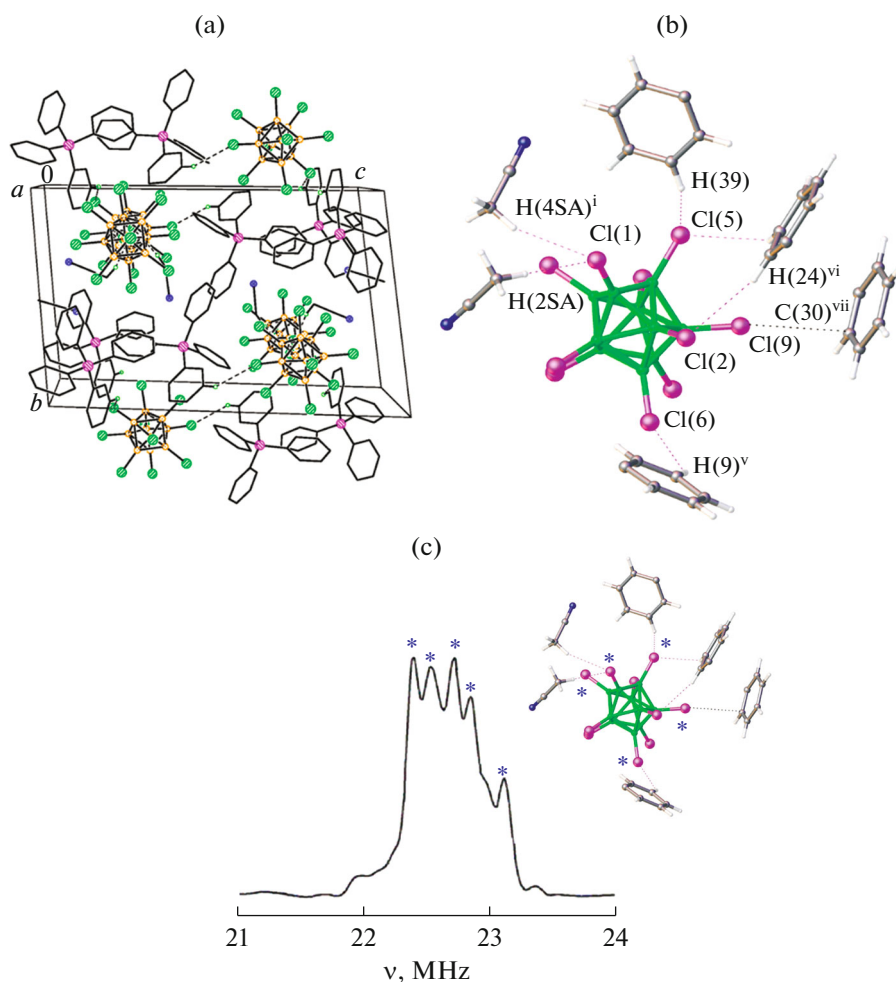
Fig. 5. Compound $(Ph_4P)_2[B_{10}Cl_{10}]\cdot 3CH_3CN$: (a) fragment of the structure, (b) environment of the boron cluster; (c) ^{35}Cl NQR spectrum. Asterisk shows contacts reflected in the ^{35}Cl NQR spectrum.

tion is observed and the compound decomposes upon heating above 440 K.

Cobalt(II) complexes. When carrying out cobalt(II) complexation reactions in the presence of organic ligands L, in contrast to iron(II) complexes, the effect of the ratio of the reaction components (metal : ligand) on the composition and structure of the final reaction products was found [44].

The reaction between cobalt chloride, $(Et_3NH)_2[B_{10}Cl_{10}]$, and a threefold excess of Phen or Bipy in CH_3CN or DMF gives a yellow tris-chelate complex $[CoL_3][B_{10}Cl_{10}]$. The reaction proceeds according to the scheme:

$$(Et_3NH)_2[B_{10}Cl_{10}] + CoCl_2 + 3Phen$$
$$\rightarrow [Co(Phen)_3][B_{10}Cl_{10}].$$
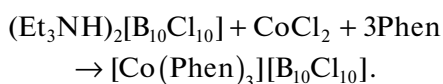
The structure of complex $[Co(Phen)_3][B_{10}H_{10}]\cdot CH_3CN$ is shown in Fig. 8. The complex consists of complex cations $[Co(Phen)_3]^{2+}$ and the $[B_{10}Cl_{10}]^{2-}$

anions. The boron cluster anions form the outer sphere of the compound.

Under the same conditions, a twofold excess of the Phen ligand with respect to cobalt leads to the formation of a binuclear cobalt(II) complex with chlorine atoms as bridging ligands $[Co_2(Phen)_4Cl_2][B_{10}Cl_{10}]$ [44] (Fig. 9). The complex precipitate from the reaction solution in the form of pink crystals according to the scheme:

$$(Et_3NH)_2[B_{10}Cl_{10}] + CoCl_2 + 2Phen$$
$$\rightarrow [Co_2(Phen)_4Cl_2][B_{10}Cl_{10}].$$
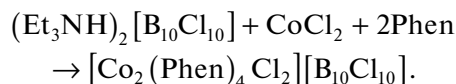
In the binuclear complex $[(Phen)_2Co(Cl_2)Co-(Phen)_2][B_{10}Cl_{10}]$, the cobalt atoms are in an octahedral environment formed by two phenanthroline molecules and chlorine atoms, which connect cobalt atoms to each other. The boron cluster anion is in the outer sphere.

Solvent molecules can participate as ligands in the formation of complex cations. This fact should be
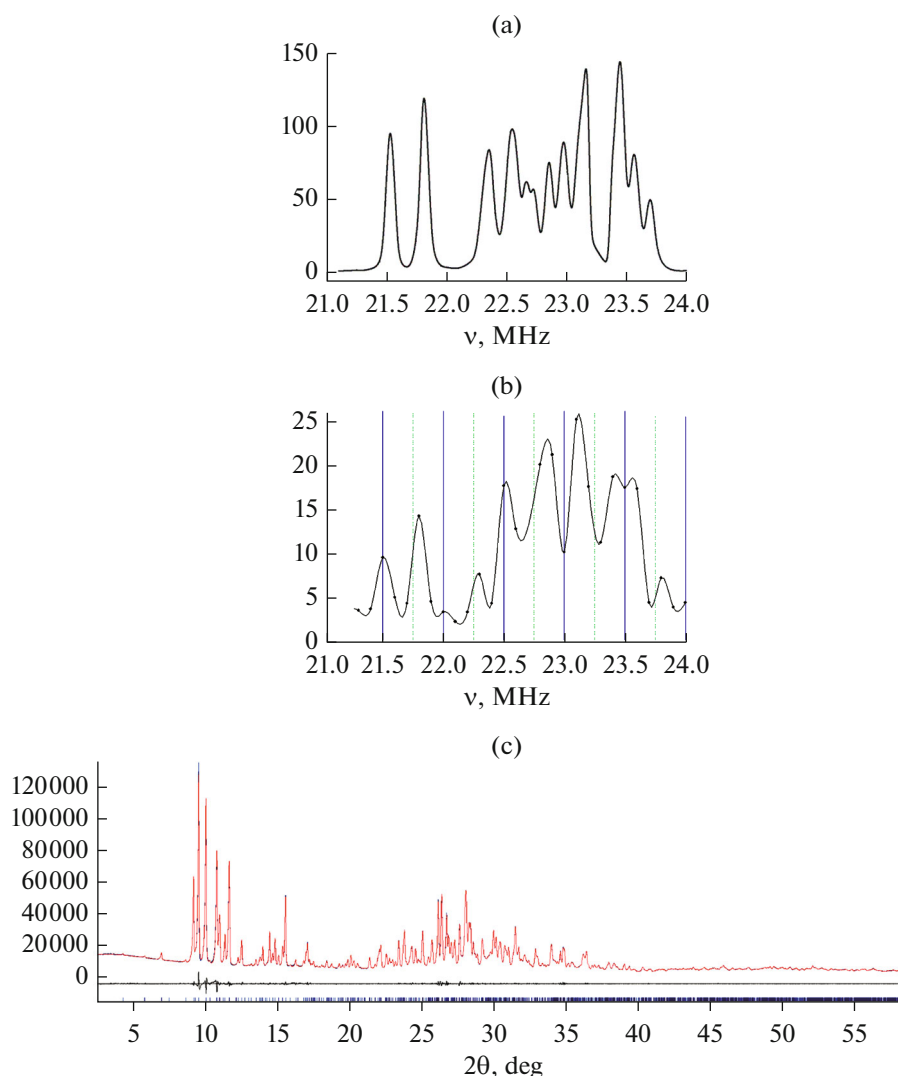
Fig. 6. ^{35}Cl NQR spectrum of salt $(Et_3NH)_2[B_{10}Cl_{10}]$ at (a) 19 and (b) 77 K; (c) X-ray powder diffraction pattern of salt $(Et_3NH)_2[B_{10}Cl_{10}]$.

taken into account when carrying out complexation reactions in solutions: the greater affinity of the complexing metal for the solvent molecules can lead to the fact that the present ligand remains unreacted. Complexes of the general formula $[Co(solv)_6][B_{10}Cl_{10}]$ (solv = CH_3CN, DMF, DMSO) were described [50]. They are formed as poorly soluble crystals when $(Et_3NH)_2[B_{10}Cl_{10}]$ was allowed to react with cobalt chloride $CoCl_2$ or cobalt nitrate $Co(NO_3)_2$ in the appropriate solvents:

$$(Et_3NH)_2[B_{10}Cl_{10}] + CoX_2\,(X = Cl, NO_3)$$
$$\xrightarrow{\text{solv}} [Co(solv)_6][B_{10}Cl_{10}]\ (solv = CH_3CN, \text{DMF, DMSO}).$$
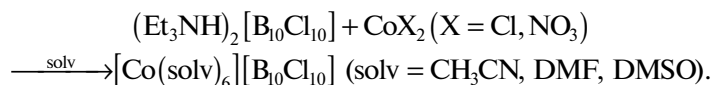
The structures of compounds $[Co(solv)_6][B_{10}Cl_{10}]$ were established by X-ray diffraction (Fig. 10) [50]. The crystals of the complexes are built of cations $[Co(solv)_6]^{2+}$ and anions $[B_{10}Cl_{10}]^{2-}$. Dimethylformamide molecules in the cationic cobalt(II) complex are disordered; Fig. 10b shows one of their positions.

Cobalt complexes were studied by EPR spectroscopy. The spectra of high-spin cobalt ions in an octahedral environment are an unsplit line with the effective spin $S = 1/2$ and isotropic g factor of 4.33. However, in the compounds under study, the octahedral environment is distorted; therefore, a rhombic split
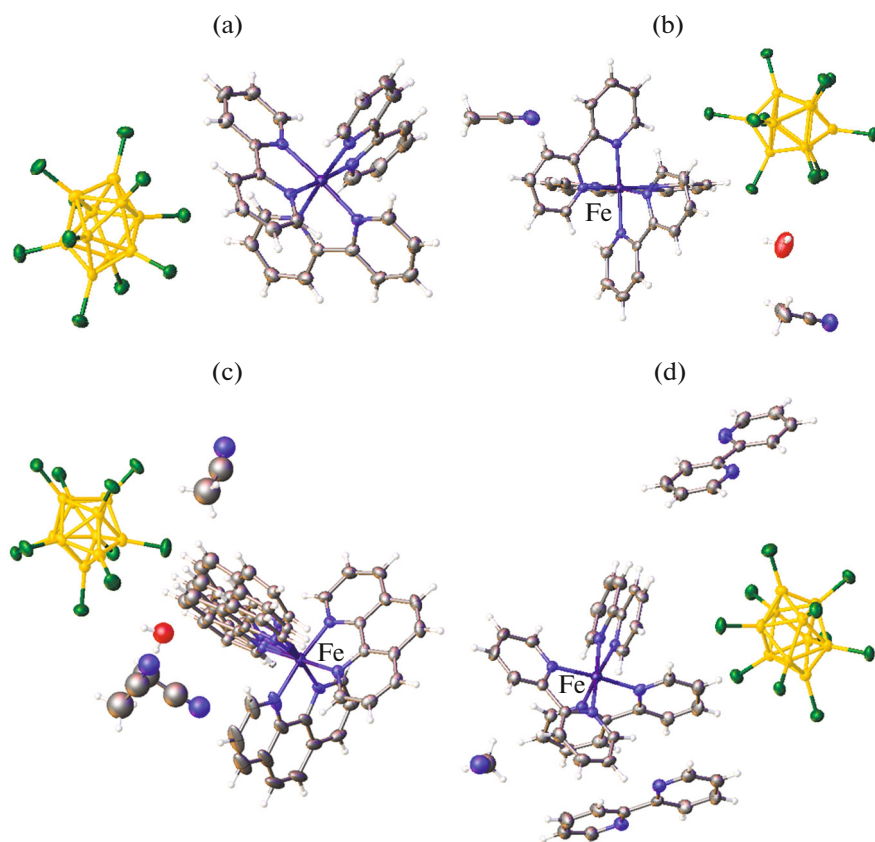
Fig. 7. Structures of complexes (a) [Fe(Bipy)$_3$][B$_{10}$Cl$_{10}$]·CH$_3$CN (CH$_3$CN molecules are omitted), (b) [Fe(Bipy)$_3$]-[B$_{10}$Cl$_{10}$]·2CH$_3$CN·H$_2$O, (c) [Fe(Phen)$_3$][B$_{10}$Cl$_{10}$]·0.88CH$_3$CN·0.12 H$_2$O, (d) [Fe(Bipy)$_3$][B$_{10}$Cl$_{10}$]·2Bipy·CH$_3$CN.
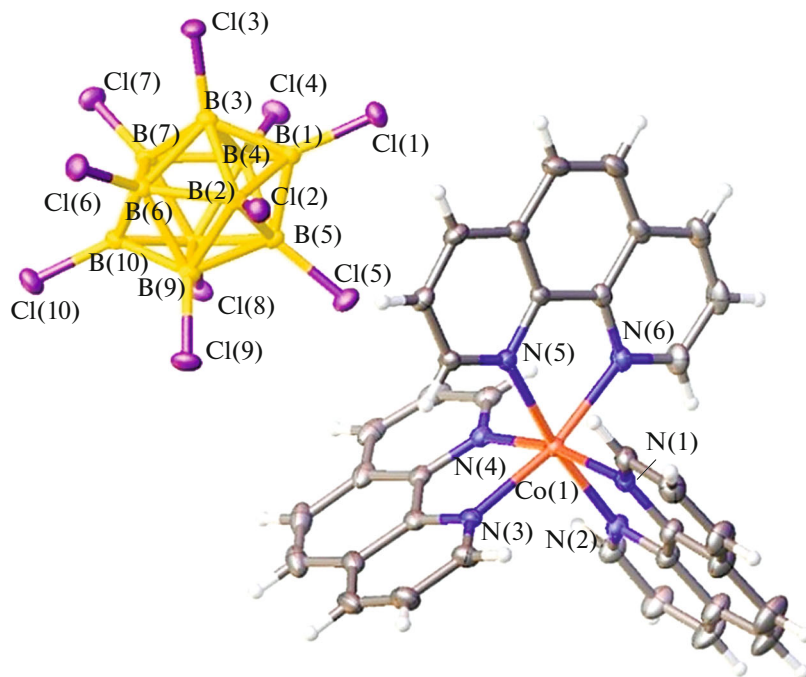
Fig. 8. Structure of complex [Co(Bipy)$_3$][B$_{10}$H$_{10}$]·CH$_3$CN. Solvent molecules are omitted.
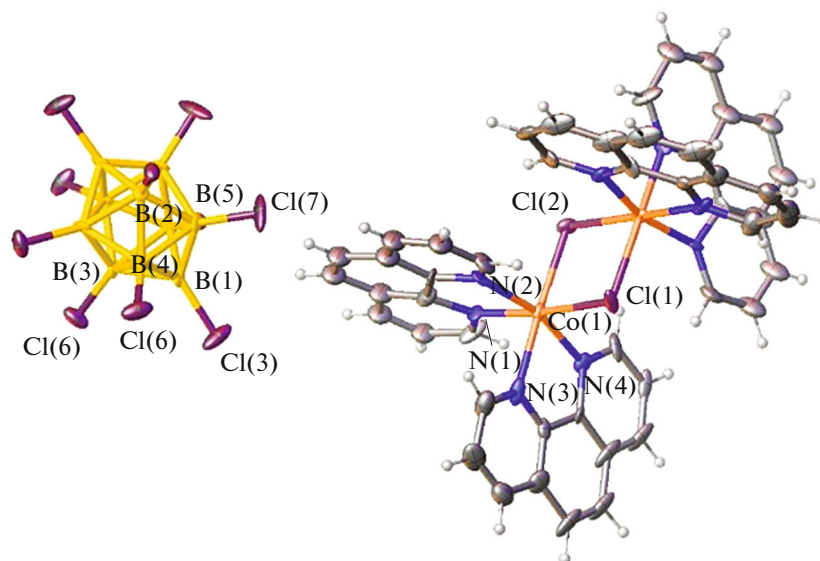
Fig. 9. Structure of $[Co_2(Phen)_4Cl_2][B_{10}Cl_{10}]\cdot CH_3CN$. Solvent molecules are omitted.

line of the effective spin $S_{eff} = 1/2$ is observed. The structure closest to the octahedron is observed for compound $[Co(DMF)_6][B_{10}Cl_{10}]$ [50] (Fig. 11).

In [51], the synthesis and structure of the pseudo-clathrochelate cobalt complex $[Co\text{-}(PzOx)_3(BC_6H_5)\text{-}DMF]_2[B_{10}Cl_{10}]$ were described. The compound was obtained by reacting 2-acetylpyrazoloxime PzOxH and phenylboronic acid with the above-described complex $[Co(DMF)_6][B_{10}Cl_{10}]$. According to X-ray diffraction data, the compound contains two independent cobalt(II) cations in the high-spin state $[Co\text{-}(PzOx)_3(BC_6H_5)DMF]^+$ (Co–N 2.115(4)–2.198(3) Å), the $[B_{10}Cl_{10}]^{2-}$ anion, solvate molecules of benzene and dichloromethane, and two molecules of DMF, which are linked to monocapped tris-pyrazole

oxime ligands via the N–H...O hydrogen bonds (Fig. 12). The data on the magnetic susceptibility of the compound were described; it was found that the compound exhibits high magnetic anisotropy. The results of magnetometric studies in an alternating magnetic field suggest that this complex exhibits the properties of a molecular magnet with an effective magnetization reversal barrier of ~130 cm^{-1}.

**Nickel(II) complexes.** Nickel(II) complexes $[Ni\text{-}(DMF)_6][B_{10}Cl_{10}]$ and $[Ni(DMSO)_6][B_{10}Cl_{10}]$ [50], similar to the above described cobalt(II) complexes, are formed by the interaction between salt $(Et_3NH)_2[B_{10}Cl_{10}]$ and nickel chloride or nickel nitrate in DMF or DMSO, respectively.

$$(Et_3NH)_2[B_{10}Cl_{10}] + NiX_2 \ (X = Cl, NO_3)$$
$$\xrightarrow{\text{DMF or DMSO}} [Ni(solv)_6][B_{10}Cl_{10}] \ (solv = DMF, DMSO)$$
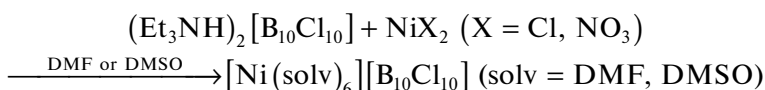
The IR spectra of complexes $[Ni(DMF)_6][B_{10}Cl_{10}]$ and $[Ni(DMSO)_6][B_{10}Cl_{10}]$ contain bands assigned to the stretching vibrations of the corresponding coordinated solvent molecules (cm^{-1}): $\nu(CO)$ at ~1640 (DMF) and $\nu(SO)$ at ~1004 (DMSO). The spectrum of $[Ni(DMF)_6][B_{10}Cl_{10}]$ contains two bands of the stretching vibrations $\nu(BCl)$ of the apical and equatorial B–Cl groups with maxima at 1015 and 1157 cm^{-1}, respectively. The structure of complex $[Ni(DMF)_6]$-$[B_{10}Cl_{10}]$ is shown in Fig. 13a.

The formation of tris-chelate nickel(II) complexes with azaheterocyclic ligands L and boron cluster anions $[B_{10}Cl_{10}]^{2-}$ of the general formula $[NiL_3][B_{10}Cl_{10}]$

(L = Bipy, Phen) was described [50]. Compounds are formed when the above-described complexes $[Ni(solv)_6][B_{10}Cl_{10}]$ was allowed to react with ligands L in the $CH_3CN–H_2O$ or $DMF–H_2O$ system according to the scheme:

$$[Ni(solv)_6][B_{10}Cl_{10}] + 3L \rightarrow [NiL_3][B_{10}Cl_{10}]$$
$$(L = Bipy \ or \ Phen).$$
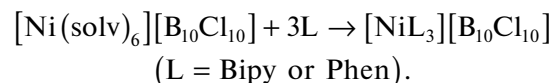
The obtained compounds precipitated as solvates from the corresponding reaction solutions. The target compounds can be synthesized in the course of solid-phase synthesis during the mechanical activation of the solid components of the reaction [50]. The struc-
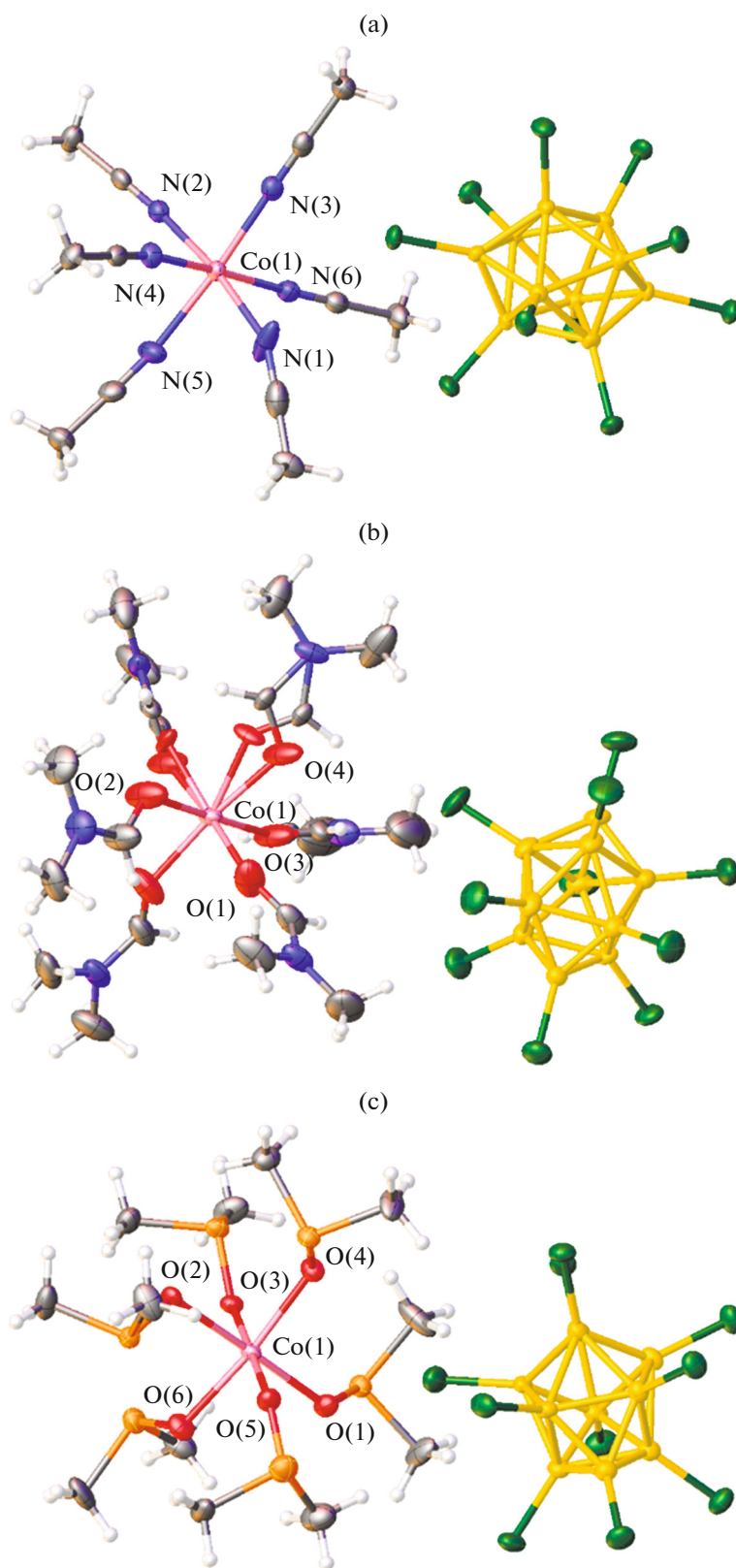
(a)

(b)

(c)

Fig. 10. Fragment of the structure of [Co(solv)$_6$][B$_{10}$Cl$_{10}$] (solv = (a) CH$_3$CN, (b) DMF, (c) DMSO).

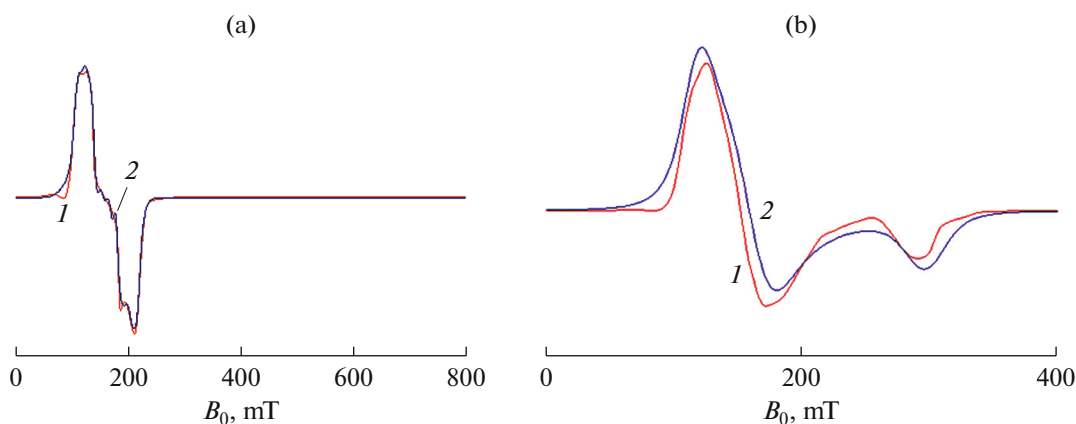**Fig. 11.** (a) EPR spectrum of powder $[Co(DMF)_6][B_{10}Cl_{10}]$ at $T = 4.5$ K: (*1*) experiment, (*2*) simulation with SG parameters ($g_z = 4.108$, $g_x = 4.052$, $g_y = 4.201$, $A = 2.852 \times 10^{-2}$ cm^{-1}, $B = 2.055 \times 10^{-2}$ cm^{-1}, $C = 1.072 \times 10^{-2}$ cm^{-1}); (b) EPR spectrum of powder $[Co(Phen)_3][B_{10}Cl_{10}]$ at $T = 8$ K: (*1*) experiment, (*2*) simulation with SG parameters: $g_z = 5.61$, $g_x = 4.20$, $g_y = 2.26$.

ture of crystals $[Ni(Phen)_3][B_{10}Cl_{10}]\cdot DMF$ was established by X-ray diffraction. The compound is built of complex cations $[Ni(Phen)_3]^{2+}$ and anions $[B_{10}Cl_{10}]^{2-}$. In complex cations, three bidentate coordinated ligands are located in approximately mutually perpendicular planes, forming a distorted octahedral environment of the Ni atom (Fig. 13b).

Manganese(II) complexes. The similarity of the behavior of manganese(II) salts with cobalt(II) salts in complexation reactions in the presence of the azaheterocyclic ligands and the $[B_{10}Cl_{10}]^{2-}$ anion was reported [52]. Thus, in the case of a threefold excess of the Bipy ligand with respect to the metal, complex $[Mn(Bipy)_3][B_{10}Cl_{10}]$ precipitated [52]. Due to the good solubility of the starting reagents in organic solvents, the reaction was carried out in DMF or CH$_3$CN:

$$(Et_3NH)_2[B_{10}Cl_{10}] + MnCl_2 + 3Bipy$$
$$\rightarrow [Mn(Bipy)_3][B_{10}Cl_{10}].$$
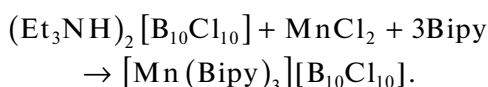
The structure of $[Mn(Bipy)_3][B_{10}Cl_{10}]$ was studied by X-ray diffraction. The complex consists of complex cations $[Mn(Bipy)_3]^{2+}$ and the perchlorinated boron anions. The structure of the compound is shown in Fig. 14a.

A decrease in the metal : ligand ratio to 1 : 2, as in the case of cobalt(II), leads to the release of a binuclear cationic manganese(II) complex with bridging chlorine atoms [52]:

$$(Et_3NH)_2[B_{10}Cl_{10}] + MnCl_2 + 2Bipy$$
$$\rightarrow [Mn_2(Bipy)_4Cl_2][B_{10}Cl_{10}].$$
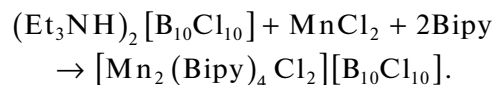
The similarity of the color of mono- and binuclear manganese(II) complexes (crystals $[Mn(Bipy)_3][B_{10}Cl_{10}]$ are bright yellow, crystals $[Mn_2(Bipy)_4Cl_2][B_{10}Cl_{10}]$ are lemon yellow), as well as the uniformity of their IR spectra (the presence of the band of stretching vibrations $\nu(B-Cl)$ at 1158 and 1004 cm^{-1}) did not allow the authors to distinguish these two manganese complexes at the first stage of the study. The different composition of the complexes was determined based on elemental analysis data and subsequently confirmed by X-ray diffraction. The structure of complex $[Mn_2(Bipy)_4Cl_2][B_{10}Cl_{10}]$ is shown in Fig. 14b.

Copper(II) complexes. In the course of complexation reactions of copper(II) sulfate in the presence of a threefold excess of the Bipy ligand in acetonitrile, tris-chelate complex $[Cu(Bipy)_3][B_{10}Cl_{10}]$ was formed [53].

$$(Et_3NH)_2[B_{10}Cl_{10}] + CuSO_4 + 3Bipy \xrightarrow{\text{CH}_3\text{CN}} [Cu(Bipy)_3][B_{10}Cl_{10}]\cdot 2CH_3CN.$$
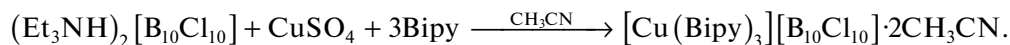
It was found by X-ray diffraction analysis that compound $[Cu(Bipy)_3][B_{10}Cl_{10}]\cdot 2CH_3CN$ contains two crystallographically nonequivalent complex cations $[Cu(Bipy)_3]^{2+}$, the $[B_{10}Cl_{10}]^{2-}$ anion, and four acetonitrile molecules (Fig. 15a). The perchlorinated $[B_{10}Cl_{10}]^{2-}$ anion acts as a counterion. As in other

compounds with the $[B_{10}Cl_{10}]^{2-}$ anion, a number of specific Cl...H interactions were found based on the X-ray diffraction data obtained.

An increase in the content of the organic ligand in the reaction solution leads to the formation of cocrystal $[Cu(Bipy)_3][B_{10}Cl_{10}]\cdot 2Bipy$ [53]:
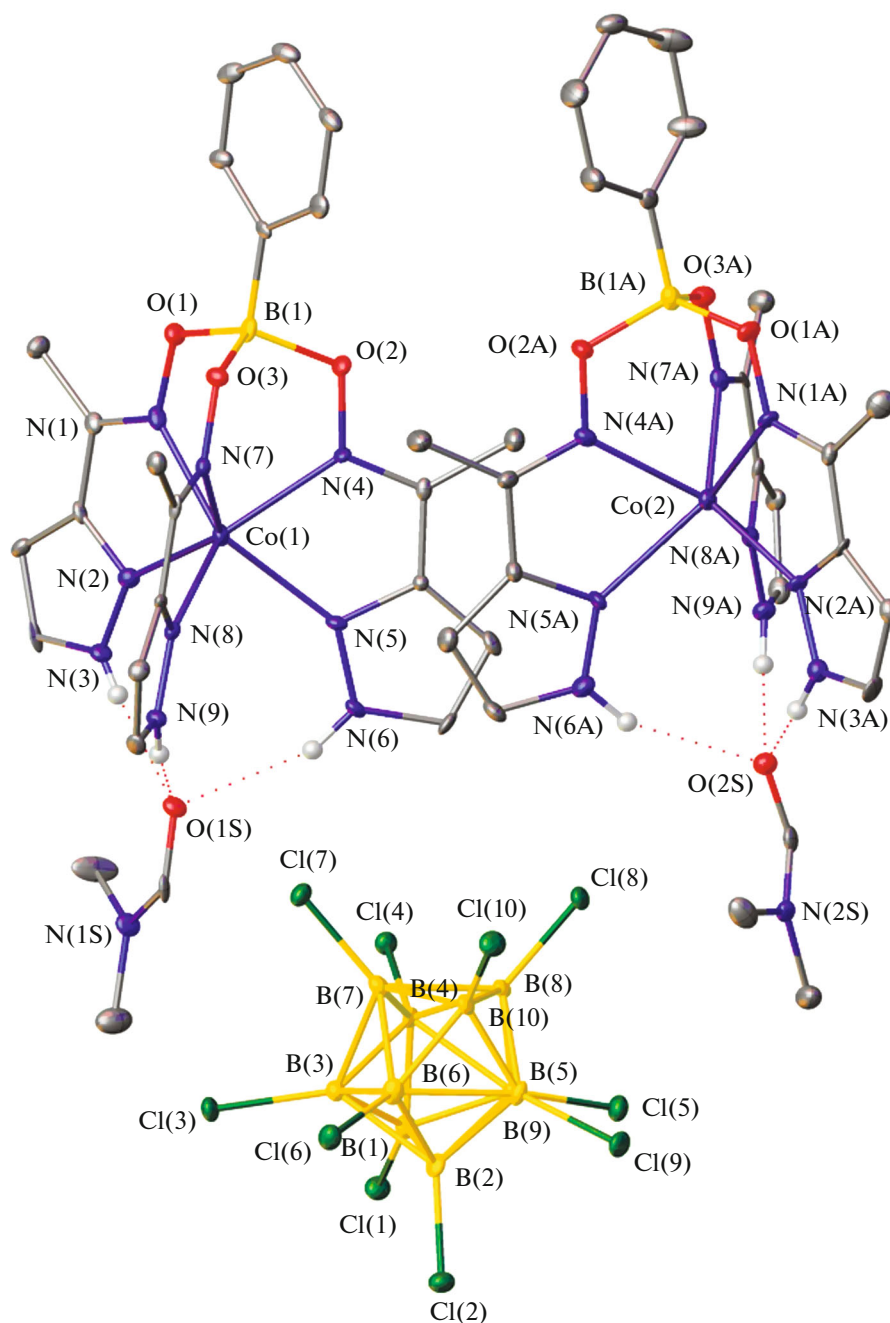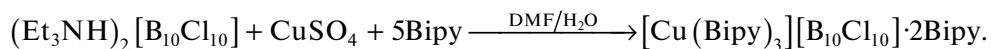
Fig. 12. Structure of pseudoclathrochelate $[Co-(PzOx)_3(BC_6H_5)DMF]_2[B_{10}Cl_{10}]$.

$$(Et_3NH)_2[B_{10}Cl_{10}] + CuSO_4 + 5Bipy \xrightarrow{\text{DMF/H}_2\text{O}} [Cu(Bipy)_3][B_{10}Cl_{10}]\cdot2Bipy.$$

The structure of the compound was determined by X-ray diffraction (Fig. 15b). The compound is built of the $[Cu(Bipy)_3]^{2+}$ cations, the $[B_{10}Cl_{10}]^{2-}$ anions, and two Bipy molecules.

As it was found, the nature of the ligand and counterion in copper(II) salts have a significant effect on the course of the complexation reaction, as well as the composition and structure of the final products. The
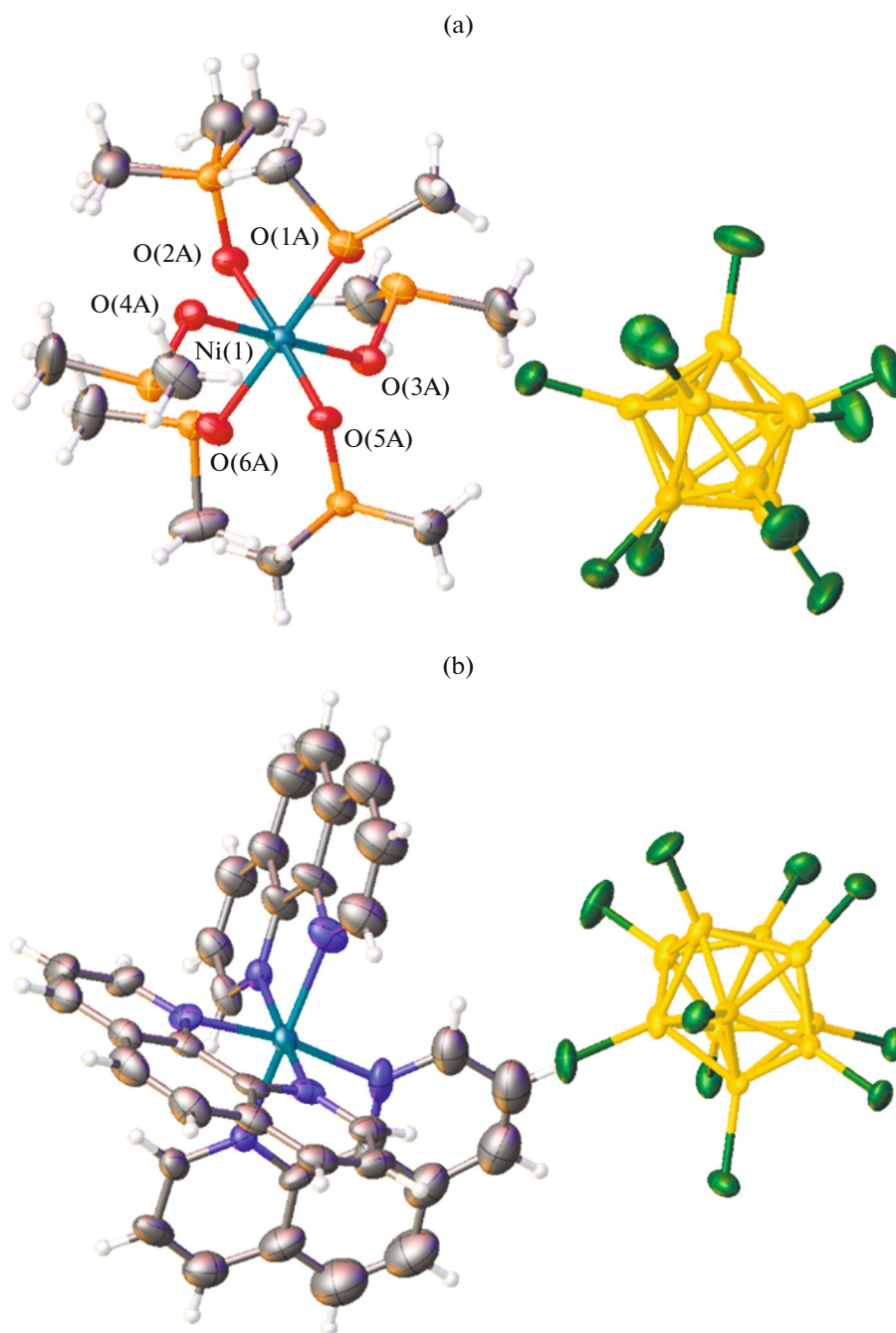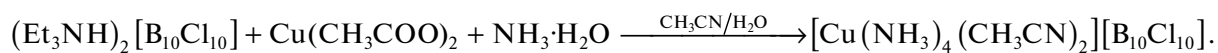
(a)

(b)

Fig. 13. Structure of nickel complexes (a) [Ni(DMF)$_6$][B$_{10}$Cl$_{10}$], (b) [Ni(Phen)$_3$][B$_{10}$Cl$_{10}$]·DMF. Solvent molecules are omitted.

interaction between aqueous solutions of copper(II) acetate and ammonia with the [B$_{10}$Cl$_{10}$]$^{2-}$ anion was studied [53]. A solution of salt (Et$_3$NH)$_2$[B$_{10}$Cl$_{10}$] in acetonitrile was added to the reaction solution containing copper(II) acetate and NH$_3$·H$_2$O. As a result of isothermal evaporation in air, crystals of mixed-ligand complex [Cu(NH$_3$)$_4$(CH$_3$CN)$_2$][B$_{10}$Cl$_{10}$] precipitated from the reaction solution.

$$(\text{Et}_3\text{NH})_2[\text{B}_{10}\text{Cl}_{10}] + \text{Cu}(\text{CH}_3\text{COO})_2 + \text{NH}_3 \cdot \text{H}_2\text{O} \xrightarrow{\text{CH}_3\text{CN}/\text{H}_2\text{O}} [\text{Cu}(\text{NH}_3)_4(\text{CH}_3\text{CN})_2][\text{B}_{10}\text{Cl}_{10}].$$
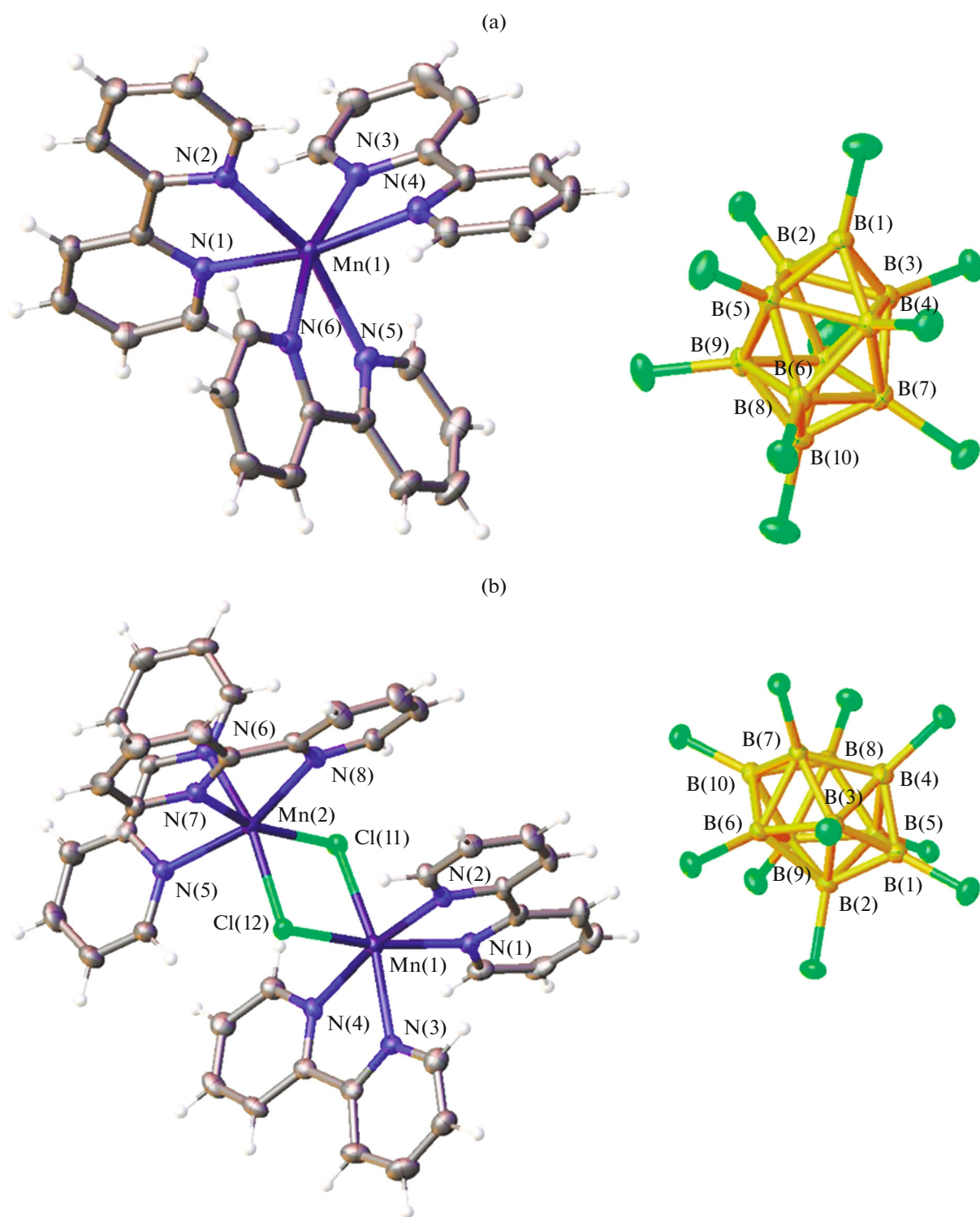
Fig. 14. Structures of (a) $[Mn(Bipy)_3][B_{10}Cl_{10}]$ and (b) $[Mn_2(Bipy)_4Cl_2][B_{10}Cl_{10}] \cdot 2CH_3CN$ (acetonitrile molecules are not shown).
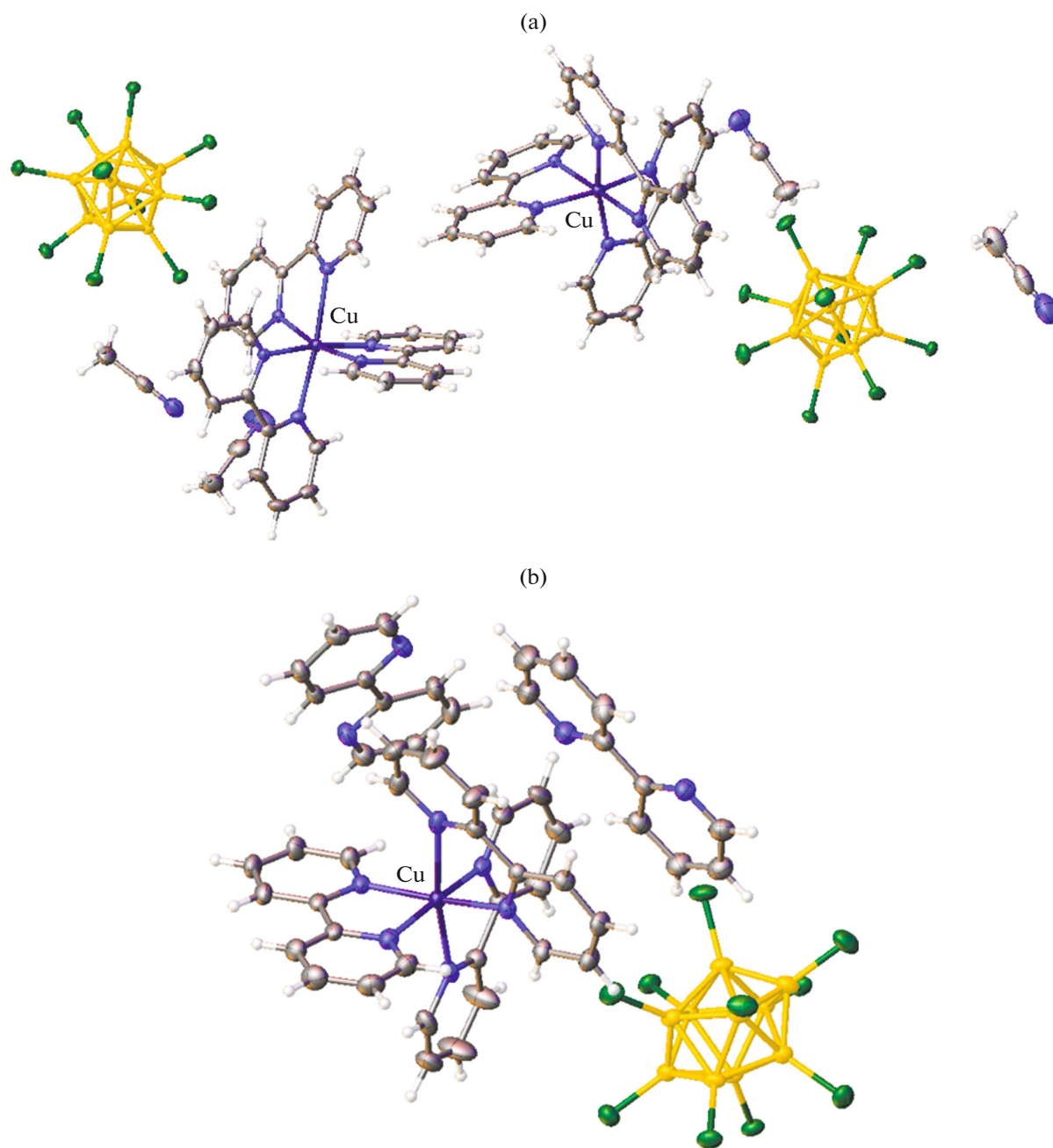
(a)

(b)

Fig. 15. Structure of (a) [Cu(Bipy)$_3$][B$_{10}$Cl$_{10}$]·2CH$_3$CN and (b) [Cu(Bipy)$_3$][B$_{10}$Cl$_{10}$]·2Bipy.

According to X-ray diffraction data, in the structure of complex [Cu(NH$_3$)$_4$(CH$_3$CN)$_2$][B$_{10}$Cl$_{10}$] (Fig. 16), the copper atom is in a square-planar environment, which is formed by the nitrogen atoms of four ammonia molecules. Two nitrogen atoms of acetonitrile molecules complete the coordination sphere of copper(II) to a distorted octahedron elongated in the axial direction. The decachloro-*closo*-decaborate anion is located in the outer sphere.

The interaction between copper(II) acetate with 1,10-phenanthroline in the presence of (Et$_3$NH)$_2$-[B$_{10}$Cl$_{10}$] in DMSO proceeds in a different way. Initially, cocrystal [CuPhen$_2$(CH$_3$CO$_2$)]$_2$[B$_{10}$Cl$_{10}$]·[CuPhen(CH$_3$CO$_2$)$_2$] is formed [54]:

$$[HNEt_3]_2[B_{10}Cl_{10}] + Cu(CH_3COO)_2 + 2Phen$$
$$\xrightarrow{\text{DMSO}} [CuPhen_2(CH_3CO_2)]_2[B_{10}Cl_{10}][CuPhen(CH_3CO_2)_2].$$

(a)

(b)
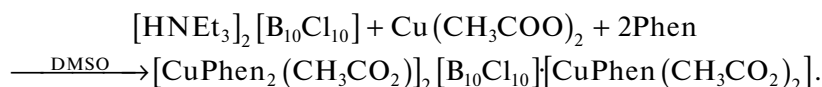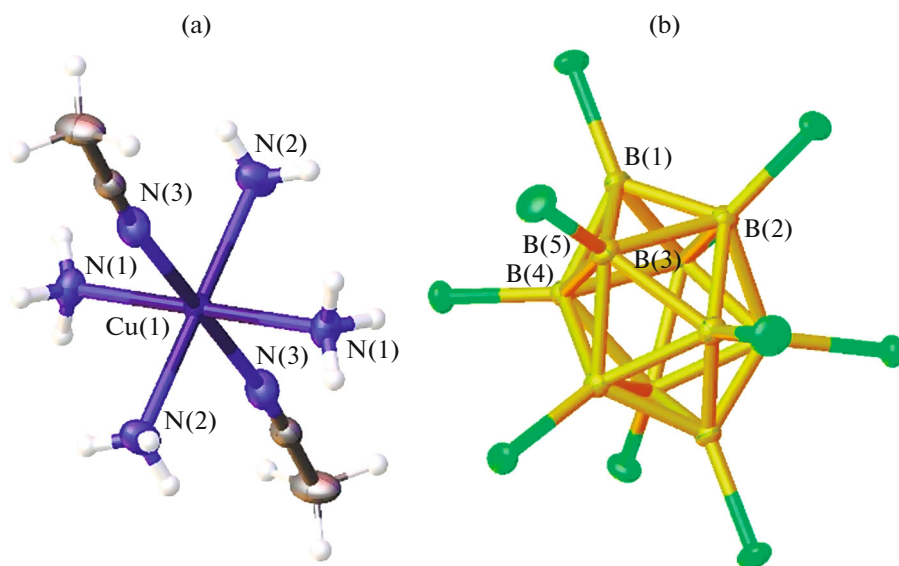
Fig. 16. Structure of $[Cu(NH_3)_4(CH_3CN)_2][B_{10}Cl_{10}]$.

(a)

(b)
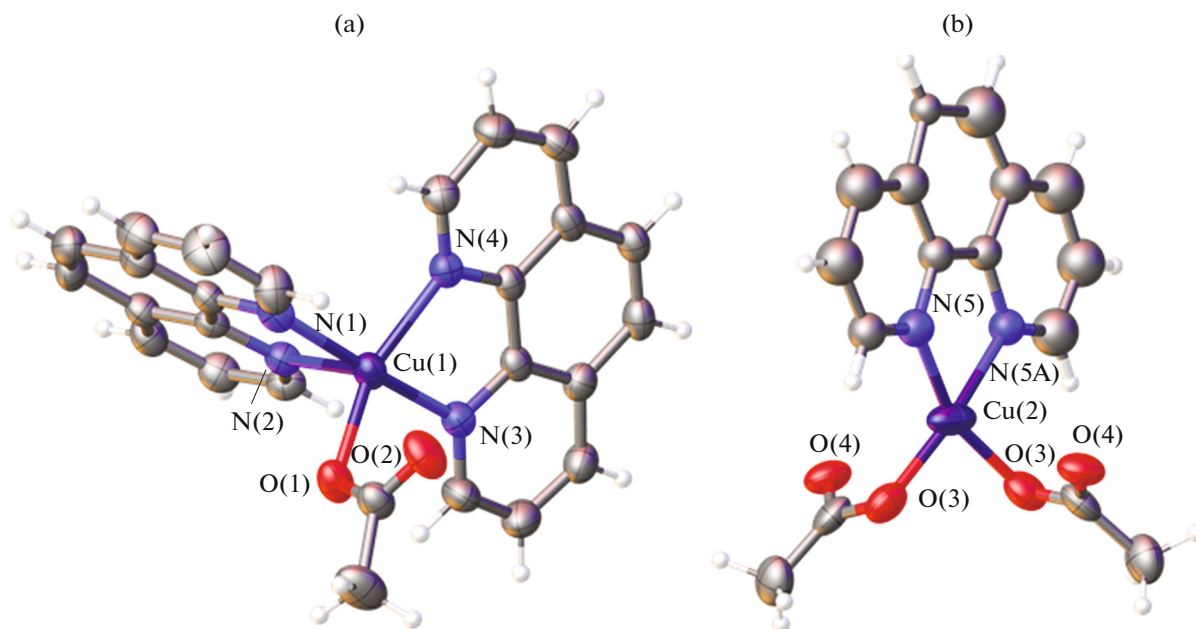
Fig. 17. Structure of copper complexes in compound $[CuPhen_2(CH_3CO_2)]_2[B_{10}Cl_{10}]\cdot[CuPhen(CH_3CO_2)_2]$.

According to X-ray diffraction data, cocrystal $[CuPhen_2(CH_3CO_2)]_2[B_{10}Cl_{10}]\cdot[CuPhen(CH_3CO_2)_2]$ consists of cationic complexes $[CuPhen_2(CH_3CO_2)]^+$, the $[B_{10}Cl_{10}]^{2-}$ anions, and neutral complexes $[CuPhen(CH_3CO_2)_2]$. The structure of the copper complexes found in the compound is shown in Fig. 17.

Both copper(II) complexes, neutral and cationic, are mononuclear.

Prolonged refluxing of the resulting compound in DMSO results in the precipitation of a complex cation with three bridging groups—two acetate groups and a hydroxo group [54]:
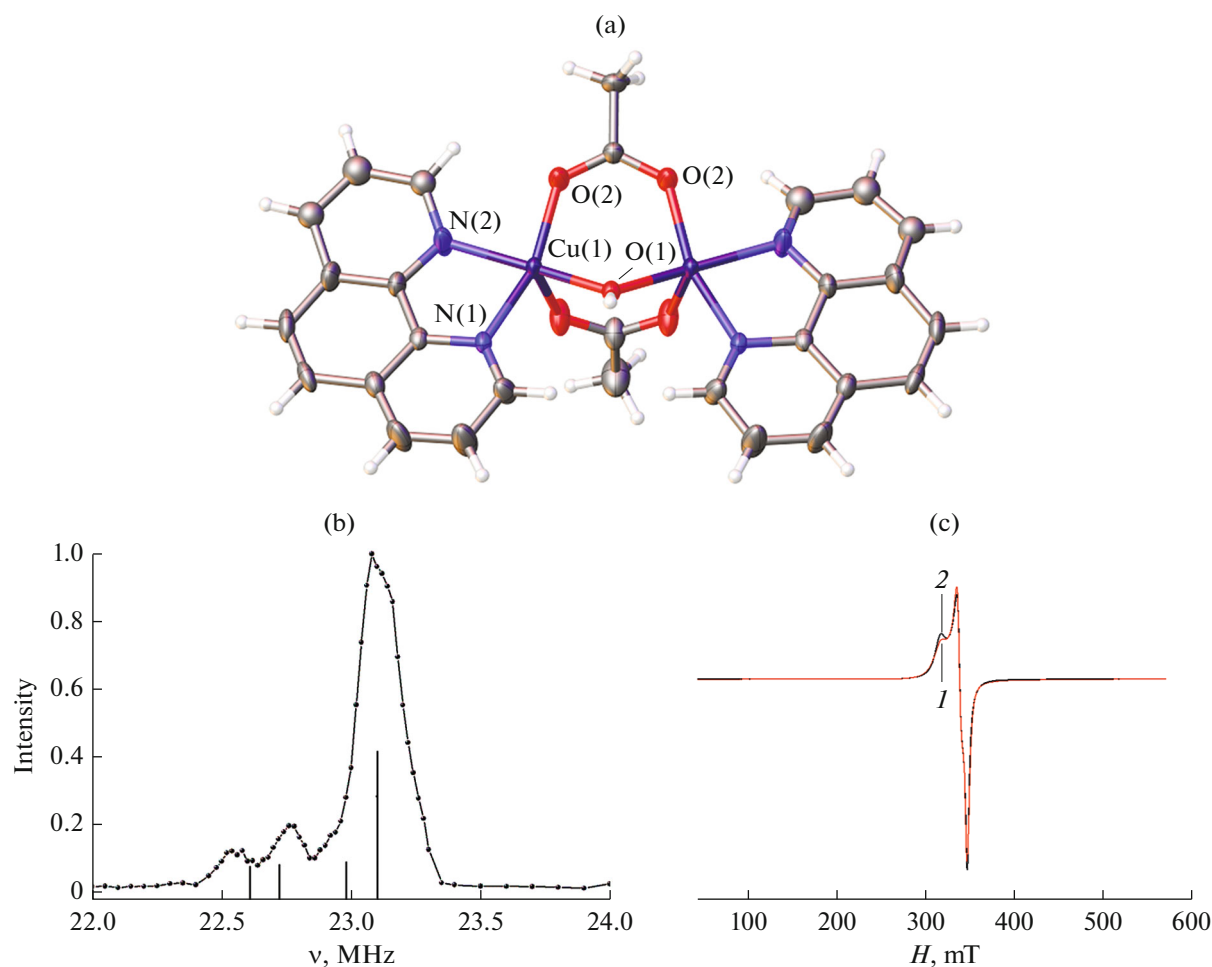
$$CuPhen_2(CH_3CO_2)]_2[B_{10}Cl_{10}]\cdot[CuPhen(CH_3CO_2)_2]$$
$$\xrightarrow{DMSO} [Cu_2Phen_2(CH_3CO_2)_2OH]_2[B_{10}Cl_{10}]\cdot3DMSO\cdot0.5H_2O.$$

(a)

(b)   (c)
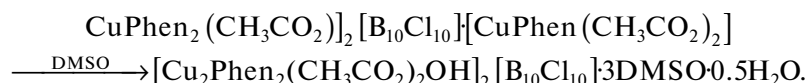
Fig. 18. Complex $[Cu_2Phen_2(CH_3CO_2)_2OH]_2[B_{10}Cl_{10}]\cdot 3DMSO\cdot 0.5H_2O$: (a) structure of the cationic part, (b) ^{35}Cl NQR spectrum at 4.2 K, (c) experimental (*1*) and theoretical (*2*) EPR spectra of a polycrystalline sample at $T = 293$ K ($g_z = 2.239$; $g_x = 2.037$; $g_y = 2.093$).

According to X-ray diffraction data (Fig. 18a), copper atoms in the binuclear cationic complex $[Cu_2Phen_2(CH_3CO_2)_2OH]^+$ are linked by two oxygen atoms from two acetate bridges and an oxygen atom of the hydroxo group. The rather short Cu...Cu distance in the dimer is 3.234(2) Å, the CuOCu angle is 116.1(3)°.

Compound $[Cu_2Phen_2(CH_3CO_2)_2OH]_2[B_{10}Cl_{10}]\cdot$ 3DMSO·0.5H₂O was studied by ^{35}Cl NQR and EPR spectroscopies [54] (Figs. 18b, 18c). The EPR spectra at $T = 293$ K are poorly resolved spectra in parallel and perpendicular orientations of the *g* tensor. Despite the presence of two copper atoms linked by three chains in the complex, there are no signs of exchange interactions between metal atoms in the spectra, namely, there is no "forbidden" transition in a half magnetic field and no line broadening in the central part of the spectrum. The EPR spectrum is typical for monomeric copper complexes with spin $S = 1/2$.

Among the complexation reactions of M(II) metals, which have several stable oxidation states and are presented in this review, we note that the interaction with copper(I) salts is accompanied by redox transformations.

When copper(I) chloride was used as the initial reagent, it was found that the complexation reaction in the presence of the azaheterocyclic ligand Bipy is accompanied by the oxidation of copper(I) to copper(II) under the action of atmospheric oxygen and the formation of a copper(II) complex as the final product [54]. When a Bipy solution in DMF is added to the reaction solution containing CuCl and $(Et_3NH)_2[B_{10}Cl_{10}]$ in the same solvent, a precipitate instantly is formed, which is the mononuclear mixed-ligand copper(II) complex $[Cu(Bipy)_2Cl]_2[B_{10}Cl_{10}]$ [54]:
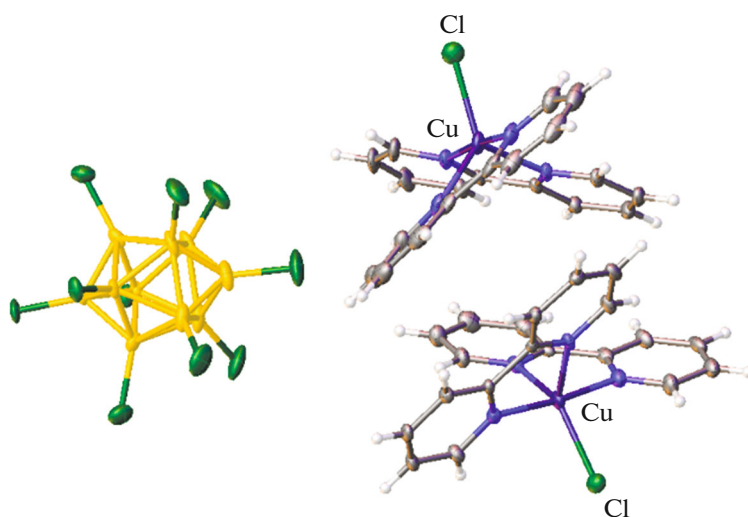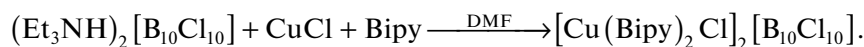
Fig. 19. Structures of (a) $[Cu(Bipy)_2Cl]_2[trans\text{-}B_{20}H_{18}]$ (one of the two cations is shown) and (b) $[Cu(Bipy)_2Cl]_2[B_{10}Cl_{10}]\cdot$2DMF (DMF molecules not shown).

$$(Et_3NH)_2[B_{10}Cl_{10}] + CuCl + Bipy \xrightarrow{\text{DMF}} [Cu(Bipy)_2Cl]_2[B_{10}Cl_{10}].$$

The recrystallization of the precipitate from DMF led to the formation of single crystals of compound $[Cu(Bipy)_2Cl]_2[B_{10}Cl_{10}]\cdot$2DMF, the structure of which is shown in Fig. 19. According to X-ray diffraction, the compound contains complex cation $[Cu(Bipy)_2Cl]^+$, the cluster anion $[B_{10}Cl_{10}]^{2-}$, and two DMF molecules.
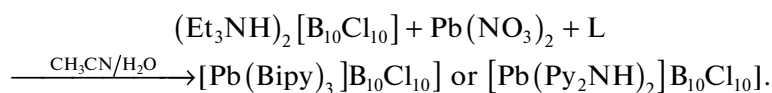
The crystal structures of copper(II) aqua complexes $[Cu(H_2O)_4][B_{10}Cl_{10}]\cdot$5H$_2$O [55] and $[Cu(H_2O)_6][B_{10}Cl_{10}]\cdot$4H$_2$O [56] formed upon neutralization of basic copper(II) carbonate with acid $[(H_3O)_2][B_{10}Cl_{10}]$ were studied:

$$(CuOH)_2CO_3 + [(H_3O)_2][B_{10}Cl_{10}]$$
$$\xrightarrow{\text{H}_2\text{O}} [Cu(H_2O)_4][B_{10}Cl_{10}]\cdot5H_2O + [Cu(H_2O)_6][B_{10}Cl_{10}]\cdot4H_2O.$$
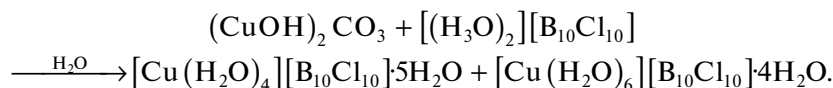
The $[Cu(H_2O)_6][B_{10}Cl_{10}]\cdot$4H$_2$O complex is built of $[Cu(H_2O)_6]^{2+}$ octahedra, which are linked by solvate water molecules into endless chains, between which the boron cluster anions are located.

Lead(II) complexes. The synthesis of lead(II) complexes with 2,2'-bipyridyl and 2,2'-bipyridylamine

$[Pb(Bipy)_3]B_{10}Cl_{10}]$ and $[Pb(Py_2NH)_2]B_{10}Cl_{10}]$ was described [57]. The compounds were synthesized by the interaction between a salt of the *closo*-decaborate anion, lead nitrate, and ligand L (L = Bipy, BPA) according to the scheme:

$$(Et_3NH)_2[B_{10}Cl_{10}] + Pb(NO_3)_2 + L$$
$$\xrightarrow{\text{CH}_3\text{CN/H}_2\text{O}} [Pb(Bipy)_3]B_{10}Cl_{10}] \text{ or } [Pb(Py_2NH)_2]B_{10}Cl_{10}].$$

According to the IR spectroscopy data, the ligands form the inner coordination sphere of the lead(II) atom.

Silver(I) complexes. The reactions of silver(I) complexation in the presence of ammonia were studied [47] and silver complex $[Ag(NH_3)_2]_2[B_{10}Cl_{10}]$ was obtained, in which the metal atom coordinates two

ammonia molecules, whereas the $[B_{10}Cl_{10}]^{2-}$ anion is located in the outer sphere. To obtain the compound, an aqueous solution of NH$_3\cdot$H$_2$O was added to an aqueous solution of $(Et_3NH)_2[B_{10}Cl_{10}]$ and AgNO$_3$:

$$(Et_3NH)_2[B_{10}Cl_{10}] + AgNO_3 + NH_3\cdot H_2O$$
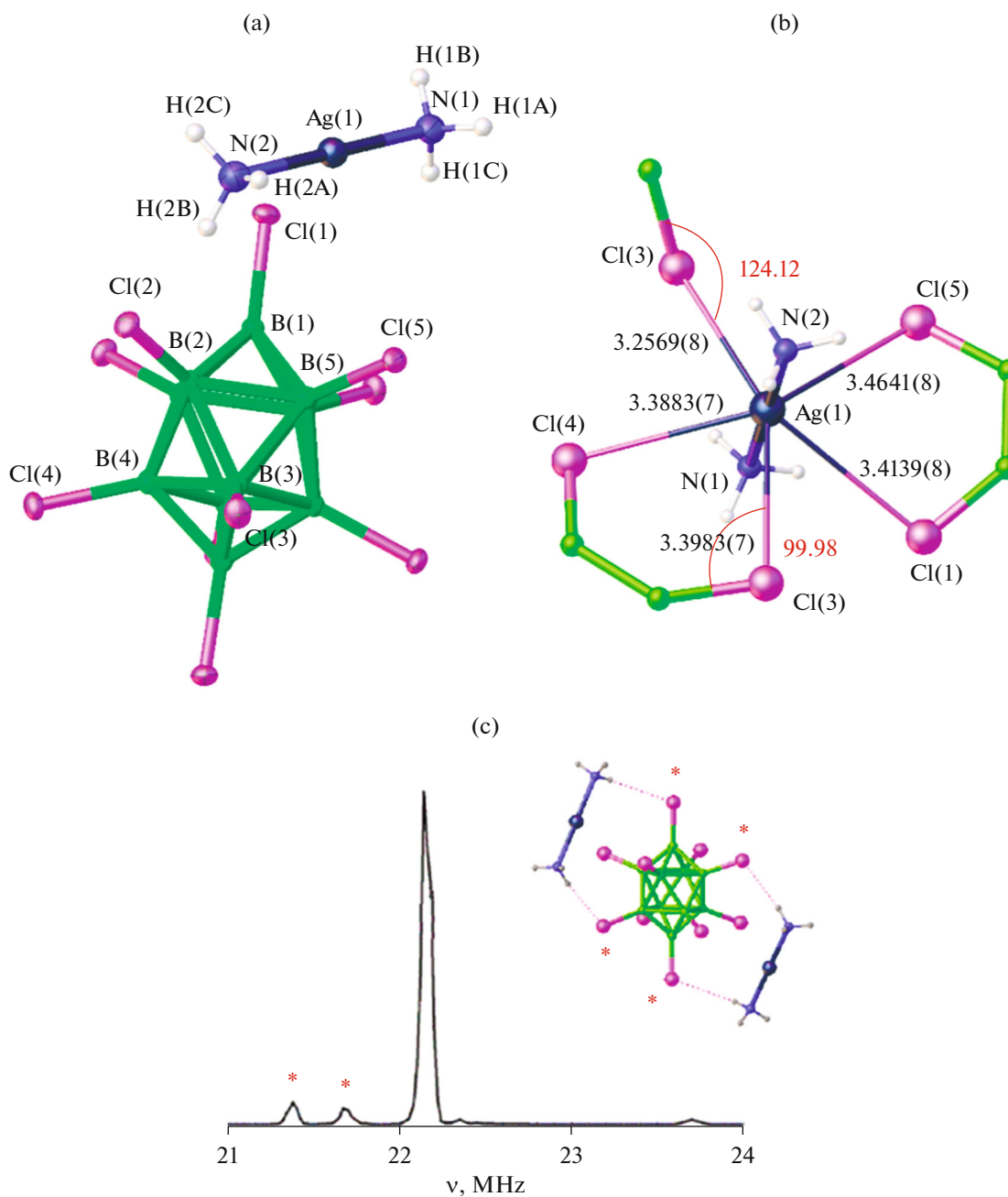$$\rightarrow [Ag(NH_3)_2]_2[B_{10}Cl_{10}].$$
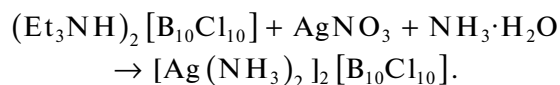
Fig. 20. Structure of [Ag(NH$_3$)$_2$]$_2$[B$_{10}$Cl$_{10}$]: (a) independent cell; (b) environment of the silver(I) atom in the structure, (c) ^{35}Cl NQR spectrum at 19 K. Asterisk shows contacts that are reflected in the ^{35}Cl NQR spectrum.

Large needle-like crystals of compound [Ag(NH$_3$)$_2$]$_2$-[B$_{10}$Cl$_{10}$] precipitated from the reaction solution. According to X-ray diffraction data (Figs. 20a, 20b), the [Ag(NH$_3$)$_2$]$^+$ cation is practically linear, the NAgN angle being 178.9°. The Ag−Cl distances in the structure fall in the range 3.257−3.464 Å. The study of X-ray diffraction data shows that for each chlorine atom, the presence of specific interactions N−H...Cl (<2.95 Å) and Ag...Cl (<3.5 Å) can be assumed. Meanwhile, the ^{35}Cl NQR spectrum (Fig. 20c) contains only three signals, which indicates a small number of specific interactions that contribute to the gradient on the chlorine atom.

When carrying out the reactions of silver(I) complexation in the presence of triphenylphosphine (Ph$_3$P), it was found that the structure of the cationic complex of silver depends on the nature of the starting reagents and the Ag : Ph$_3$P ratio. Compound [Ag$_2$(Ph$_3$P)$_3$(H$_2$O)][B$_{10}$Cl$_{10}$]·2DMF is formed by the interaction between K$_2$[B$_{10}$Cl$_{10}$] and the previously

(a)

(b)
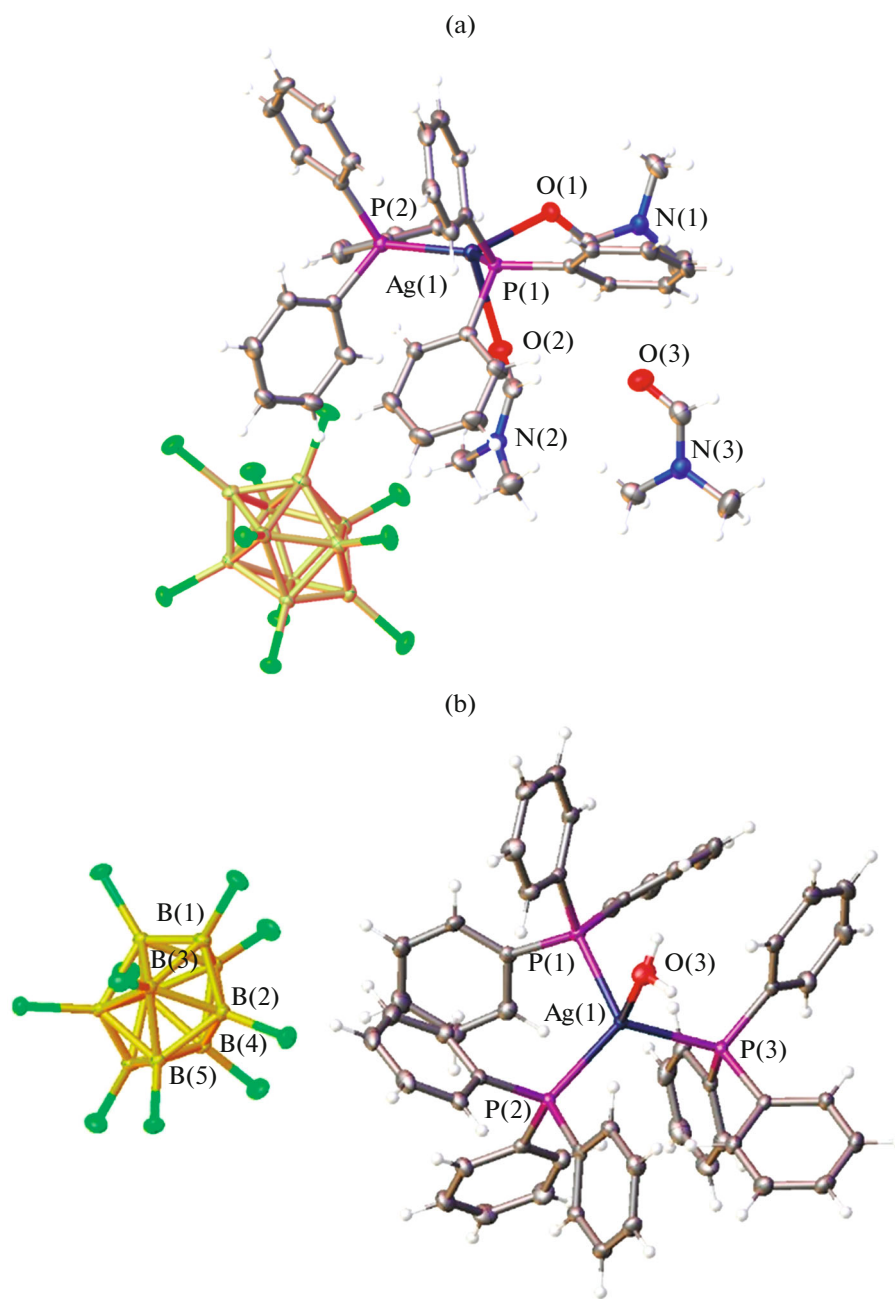
Fig. 21. Structure of silver(I) complexes (a) [Ag(PPh$_3$)$_2$(DMF)$_2$]$_2$[B$_{10}$Cl$_{10}$]·2DMF and (b) [Ag$_2$(Ph$_3$P)$_3$(H$_2$O)][B$_{10}$Cl$_{10}$]·2DMF.

obtained silver(I) complex [Ag(Ph$_3$P)$_3$NO$_3$] in the H$_2$O–DMF system. In this compound, the silver atom coordinates three triphenylphosphine molecules and a water molecule (Fig. 21a) [58]:

$$K_2\left[B_{10}Cl_{10}\right] + \left[Ag\left(Ph_3P\right)_3 NO_3\right]$$
$$\xrightarrow{\text{DMF}} \left[Ag_2\left(Ph_3P\right)_3\left(H_2O\right)\right]\left[B_{10}Cl_{10}\right]\cdot 2DMF.$$
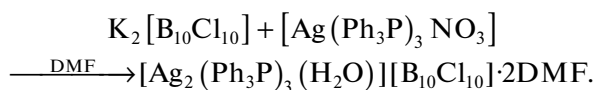
In the case of using silver(I) nitrate and free ligand Ph$_3$P as starting reagents and at a reagent ratio of Ag : Ph$_3$P equal to 1 : 2, complex [Ag(PPh$_3$)$_2$-

(DMF)$_2$]$_2$[B$_{10}$Cl$_{10}$]·2DMF was isolated from the reaction solution (Fig. 21b) [58]:

$$\left(Et_3NH\right)_2\left[B_{10}Cl_{10}\right] + 2AgNO_3 + 4Ph_3P$$
$$\xrightarrow{\text{DMF}} \left[Ag\left(PPh_3\right)_2\left(DMF\right)_2\right]_2\left[B_{10}Cl_{10}\right]\cdot 2DMF.$$
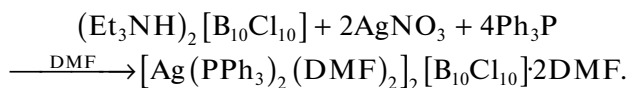
Analyzing the results obtained, the authors [58] believe that the formation of the final coordination polyhedron of the metal is determined by the coordination environment of the metal in the solution followed by the metathesis of ligands.
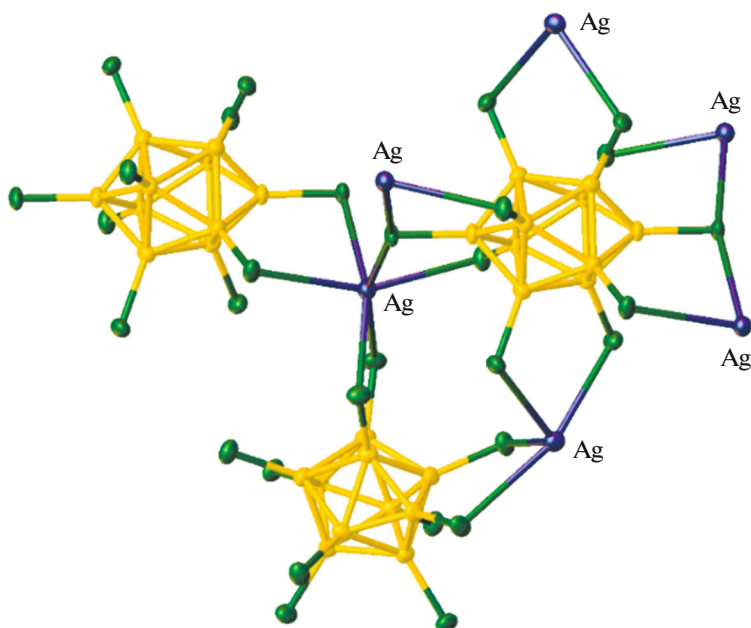
Fig. 22. Fragment of the structure of $[Ag_2[B_{10}Cl_{10}]]_n$.

Uranium(IV) complexes. In [59, 60], the uranyl aqua complexes $[UO_2(H_2O)_6][B_{10}Cl_{10}]$ were studied. It was found that the inner sphere of uranyl is formed by water molecules, while the $[B_{10}Cl_{10}]^{2-}$ boron clusters are located in the outer sphere and do not interact with the uranyl group. The authors [61] described the synthesis and structure of a similar complex with dimethyl sulfoxide of the composition $[UO_2(DMSO)_6][B_{10}Cl_{10}]$.

COMPLEX COMPOUNDS WITH COORDINATED DECACHLORO-*closo*-DECABORATE ANION

Taking into account the results described above, it is obvious that carrying out reactions of metal complexation with the $[B_{10}Cl_{10}]^{2-}$ anion in the presence of competitive ligands L leads, as a rule, to the formation of compounds with complex cations, in which the perchlorinated anions play the role of a counterion. Meanwhile, examples of silver(I) complexes with the coordinated perchlorinated *closo*-dodecaborate anion $[B_{12}Cl_{12}]^{2-}$ [62, 63] and halogenated carboranes [64–69] are known in the literature.

Carrying out the complexation reaction in the absence of competing ligands showed the possibility of obtaining compounds with the coordinated $[B_{10}Cl_{10}]^{2-}$ anion. The synthesis and structure of polymeric complex $[Ag_2[B_{10}Cl_{10}]]_n$ are described [58]. The compound is formed in an aqueous solution according to the scheme by the interaction of the corresponding salts:

$$(Et_3NH)_2[B_{10}Cl_{10}] + 2AgNO_3 \xrightarrow{\text{H}_2\text{O}} [Ag_2[B_{10}Cl_{10}]]_n.$$

Its structure was determined by X-ray diffraction. In the complex, the metal cation coordinates three boron cluster anions with the formation of five-membered Cl–B–B–Cl–Ag rings; the coordination polyhedron of the silver(I) atom is the $AgCl_6$ octahedron, the Ag–Cl distances are 2.706(1)–2.893(1) Å. In turn, each boron cluster anion is surrounded by six monocations. Four of them coordinate one apical and one equatorial chlorine atoms, and two silver atoms interact with two equatorial chlorine atoms (Fig. 22). As a result of the above interactions, the coordination polymer is formed.

When carrying out a similar reaction in acetonitrile, the possibility of synthesizing a mixed-ligand complex of polymer structure was established; in the product, the silver(I) atom coordinates the boron cluster anions and solvent molecules.

$$K_2[B_{10}Cl_{10}] + 2AgNO_3$$
$$\xrightarrow{\text{CH}_3\text{CN}} [Ag_2(CH_3CN)_2[B_{10}Cl_{10}]]_n + 2KNO_3\downarrow.$$
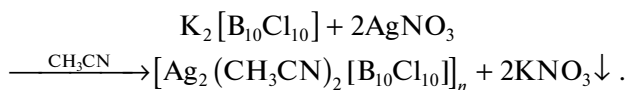
In this reaction, when the reagents are fused, potassium nitrate is instantly formed, which practically quantitatively precipitates from the reaction solution. Thus, only silver cations, boron cluster anions,
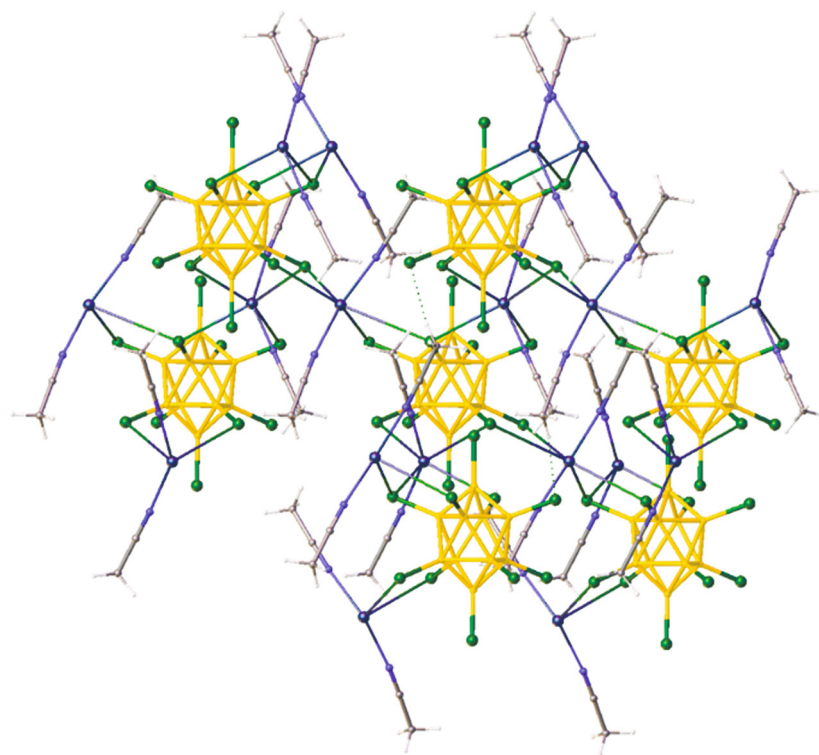
Fig. 23. Fragment of the structure of $[Ag_2(CH_3CN)_2[B_{10}Cl_{10}]]_n$.

and solvent molecules remain in the reaction solution. Isothermal evaporation of the solution leads to the selective isolation of polymeric complex $[Ag_2(CH_3CN)_2[B_{10}Cl_{10}]]_n$ [58]. According to X-ray diffraction data, the silver(I) atom coordinates two solvent molecules and two $[B_{10}Cl_{10}]^{2-}$ anions to form the AgN_2Cl_4 coordination polyhedron. Each $[B_{10}Cl_{10}]^{2-}$ anion is coordinated by four metal atoms; as a result, a three-dimensional framework structure is formed (Fig. 23).

A similar reaction in dimethylformamide leads to the formation of polymeric compound $[Ag_2[B_{10}Cl_{10}](DMF)_2]_n$ (Fig. 24) [58]:

$$(Et_3NH)_2[B_{10}Cl_{10}] + 2AgNO_3$$
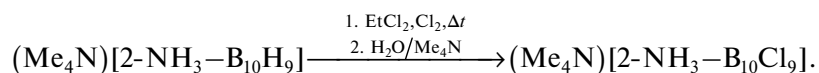$$\xrightarrow{\text{DMF}} [Ag_2[B_{10}Cl_{10}](DMF)_2]_n.$$
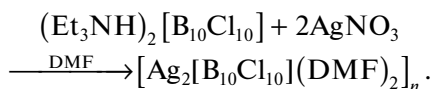
Compound $[Ag_2[B_{10}Cl_{10}](DMF)_2]_n$ is a coordination polymer built of the $[B_{10}Cl_{10}]^{2-}$ anions, silver(I) atoms, and coordinated DMF molecules (Fig. 24). Two silver(I) atoms are bonded together by DMF molecules;

the Ag–Ag distance in the crystal is 3.202 Å, and the Ag–B bond lengths are in the range 2.636–2.828 Å. The compound was studied by Raman spectroscopy. According to the data obtained, it can be assumed that the complex contains the Ag–Ag bond [58].

COMPOUNDS WITH PERCHLORINATED ANION AND SUBSTITUENTS $[B_{10}Hal_9R]^{2-}$

Recently, a method for the synthesis of a new class of compounds containing the perchlorinated *closo*-decaborate anion with substituent R introduced into the boron cage has been actively studied. To obtain them, the substituted derivatives of the decahydro-*closo*-decaborate anion $[B_{10}H_9R]^-$ containing the exo-polyhedral functional group R are chlorinated, which leads to the substitution of all hydrogen atoms by halogen atoms to form derivatives $[B_{10}Hal_9R]^-$.

Thus, chlorination of the amino-substituted *closo*-decaborate anion gives the nonachloro-*closo*-2-aminodecaborate anion [70]:

$$(Me_4N)[2-NH_3-B_{10}H_9] \xrightarrow[\text{2. H}_2\text{O/Me}_4\text{N}]{\text{1. EtCl}_2, \text{Cl}_2, \Delta t} (Me_4N)[2-NH_3-B_{10}Cl_9].$$

Note that carrying out this reaction in water leads to a number of side processes. At temperatures above

200°C, the boron cluster degrades; chlorination at room temperature leads to the formation of a number
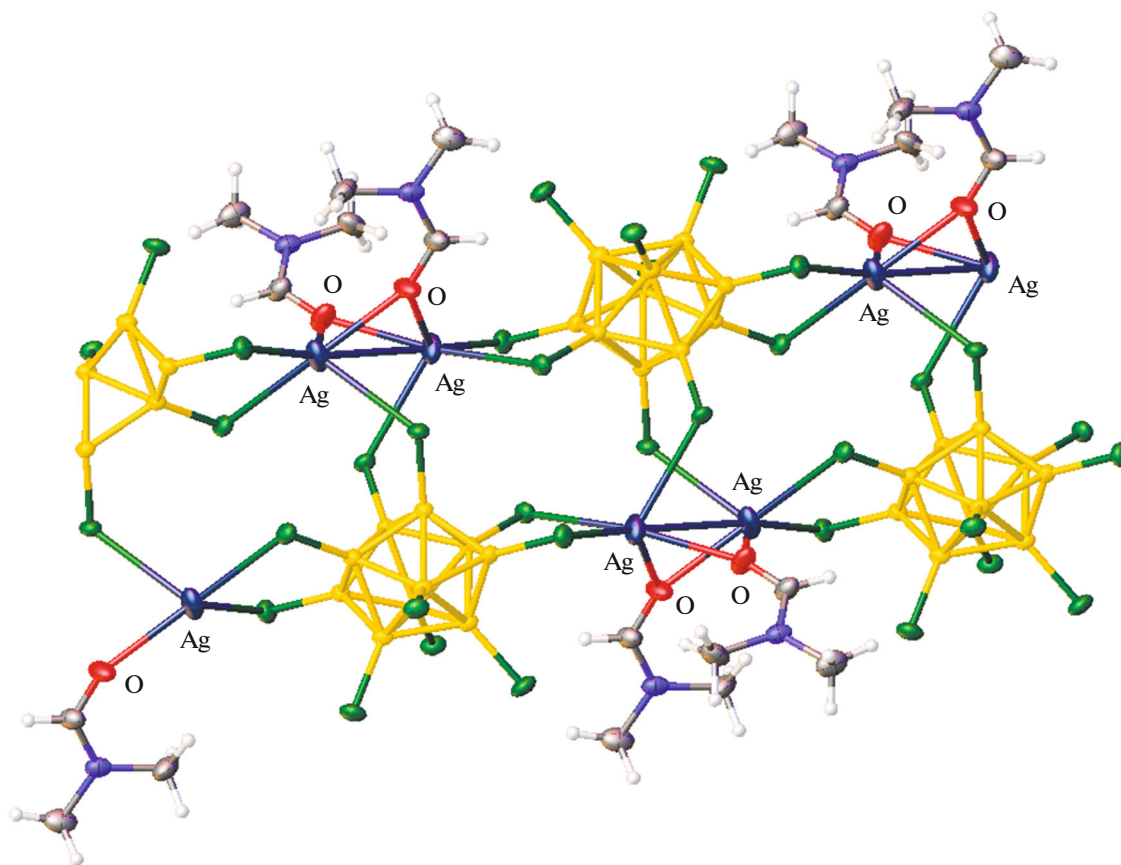
Fig. 24. Fragment of the structure of $[Ag_2[B_{10}Cl_{10}](DMF)_2]_n$.

of products with varying degrees of substitution, containing up to eight chlorine atoms; moreover, substituted derivatives containing halogen atoms and

○ C
○ H
○ B
● Cl
● N
● O

Fig. 25. Molecular structure of $Me_4N[2-NH_3-B_{10}Cl_9]\cdot H_2O$.

hydroxy groups as substituents have been found. The best way to carry out this reaction is slowly heating a suspension of $(Me_4N)[2-NH_3-B_{10}H_9]$ in dichloroethane in excess of chlorine at a temperature of -78 to 80°C for a week. The structure of the final compound is shown in Fig. 25.
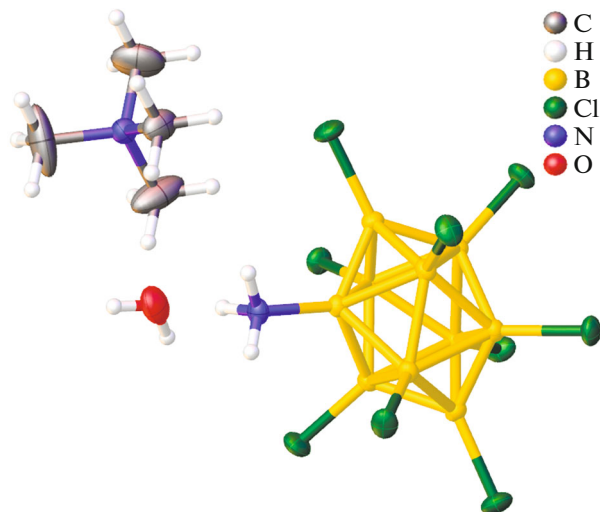
Chlorination of the $[B_{10}H_9S((CH_2)_3N(CO)_2-C_6H_4)_2]^-$ anion using SO_2Cl_2 led to the synthesis of compound $(Bu_4N)[B_{10}Cl_9S((CH_2)_3N(CO)_2C_6H_4)_2]$, the structure of which is shown in Fig. 26 [71]. In the structure of the compound, the boron cluster anions face each other by exopolyhedral substituents, and the $[B_{10}Cl_9]^-$ anions are located between the Bu_4N^+ cations. The B–S distance is 1.890(3) Å.

In conclusion, we note that substituted derivatives of boron cluster anions can actually be considered as a metal cluster that attaches a "ligand" which is a substituent molecules. This point of view was expressed by A.A. Pasynskii, who worked for many years at the Nesmeyanov Institute of Organoelement Compounds RAS and the Kurnakov Institute of General and Inorganic Chemistry RAS and always showed interest in works related to the chemistry of boron cluster anions; he urged his colleagues to find analogies in the chemical behavior of compounds of different classes [72].
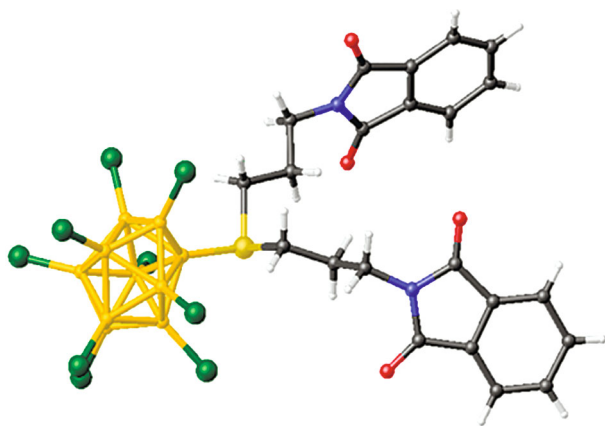
Fig. 26. Molecular structure of $(Bu_4N)[B_{10}Cl_9S-((CH_2)_3N(CO)_2C_6H_4)_2]$.

Analyzing the literature data described in this work, the following conclusions can be drawn.

(1) For most compounds containing the perchlorinated $[B_{10}Cl_{10}]^{2-}$ anion, one can expect the presence of secondary Cl...X (X = N, C, O) interactions with solvent molecules, organic ligands, and/or organic cations. The formation of this type of interaction can be identified by a combination of ^{35}Cl NQR spectroscopy and X-ray diffraction.

(2) In complex compounds of metals M(II) (Fe(II), Co(II), Ni(II), Mn(II), Cu(II)) in the presence of organic and inorganic ligands L, the perchlorinated boron cluster anions $[B_{10}Cl_{10}]^{2-}$ form an outer sphere and do not participate in the formation of coordination bonds with the metal. In these compounds, metal atoms coordinate ligands L or solvent molecules.

(3) The composition and structure of compounds with the $[B_{10}Cl_{10}]^{2-}$ anion depends on the stability of the cationic metal complexes in the reaction solution. For M(II) with a threefold excess of ligands L (Bipy, Phen), tris-chelate complexes $[ML_3][B_{10}Cl_{10}]$ were obtained. For manganese(II) and cobalt(II), it was found that a decrease in the content of ligand L with respect to the metal leads to the formation of binuclear complexes $[M_2L_4Cl_2][B_{10}Cl_{10}]$.

(4) At present, the first examples of polymeric silver complexes with the coordinated $[B_{10}Cl_{10}]^{2-}$ anion are known. The synthesis of such compounds can be realized in the absence of competitive bulky ligands. Complexes $[Ag_2[B_{10}Cl_{10}]]_n$, $[Ag_2(CH_3CN)_2[B_{10}Cl_{10}]]_n$, and $[Ag_2[B_{10}Cl_{10}](DMF)_2]_n$, which are coordination polymers with a three-dimensional framework structure, have been isolated and characterized.

(5) A method has been developed for the synthesis of a new class of compounds based on a perhalogenated 10-vertex cluster, which contain the substituted *closo*-decaborate anion $[B_{10}Cl_9R]^-$ with nine chlorine atoms and functional group R introduced. The obtained compounds provide new opportunities for studying the chemical behavior of halogenated anions and the structural features of the obtained compounds (participation in non-bonded interactions, coordination ability, etc.).

CONFLICT OF INTEREST

The authors declare that they have no conflicts of interest.

REFERENCES

1. Muetterties, E.L. and Knoth, W.H., *Polyhedral Boranes*, New York: Dekker, 1968.

2. Greenwood, N.N. and Earnshaw, A., *Chemistry of the Elements*, Butterworth-Heinemann, 1997.

3. *Boron Science: New Technologies and Applications*, Hosmane N.S., Ed., CRC Press, 2012.

4. Bruce King, R., *Chem. Rev.*, 2001, vol. 101, no. 5, p. 1119
https://doi.org/10.1021/cr000442t

5. Chen, Z. and King, R.B., *Chem. Rev.*, 2005, vol. 105, p. 3613.
https://doi.org/10.1021/cr0300892

6. Kuznetsov, N.T., Ionov, S.P., and Solntsev, K.A., *Razvitie kontseptsii aromatichnosti: poliedricheskie struktury* (Development of the Aromaticity Concept: Polyhedral Structures), Moscow: Nauka, 2009.

7. Sivaev, I.B., *Chem. Heterocycl. Comp.*, 2017, vol. 53, p. 638.
https://doi.org/10.1007/s10593-017-2106-9

8. Knoth, W.H., *Polyamides and Polyesters of Polyhedral Boron Compounds*, US Patent 3354121.

9. Skachkova, V.K., Grachev, A.V., Goeva, L.V., et al., RF Patent 2550156 C1, 2015.

10. Goswami, L.N., Ma, L., Chakravarty, Sh., et al., *Inorg. Chem.*, 2013, vol. 52, p. 1694.
https://doi.org/10.1021/ic3017613

11. Plesek, J., *Chem. Rev.*, 1992, vol. 92, p. 269.
https://doi.org/10.1021/cr00010a005

12. Sivaev, I.B., Bregadze, V.I., and Kuznetsov, N.T., *Russ. Chem. Bull.*, 2002, vol. 51, p. 1362.
https://doi.org/10.1023/A:1020942418765

13. Sivaev, I.B. and Bregadze, V.I., *Eur. J. Inorg. Chem.*, 2009, p. 1433.
https://doi.org/10.1002/ejic.200900003

14. Teixidor, F., Viñas, C., Demonceau, A., and Núñez, R., *Pure Appl. Chem.*, 2003, vol. 75, p. 1305.
https://doi.org/10.1351/pac200375091305

15. Kuznetsov, N.T., *Russ. J. Inorg. Chem.*, 2002, vol. 47, suppl. 1, p. 68.

16. Zhizhin, K.Yu., Zhdanov, A.P., and Kuznetsov, N.T., *Russ. J. Inorg. Chem.*, 2010, vol. 55, no. 14, p. 2089.
https://doi.org/10.1134/S0036023610140019

17. Sivaev, I.B., Prikaznov, A.V., and Naoufal, D., *Collect. Czech. Chem. Commun.*, 2010, vol. 75, no. 11, p. 1149.
https://doi.org/10.1135/cccc2010054

18. Sivaev, I.B., Bregadze, V.I., and Sjöberg, S., *Collect. Czech. Chem. Commun.*, 2002, vol. 67, p. 679.
https://doi.org/10.1135/cccc20020679

19. Avdeeva, V.V., Malinina, E.A., Sivaev, I.B., et al., *Crystals*, 2016, p. 6, article 60.
https://doi.org/10.3390/cryst6050060

20. Malinina, E.A., Avdeeva, V.V., Goeva, L.V., et al., *Russ. J. Inorg. Chem.*, 2010, vol. 55, no. 14, p. 2148.
https://doi.org/10.1134/S0036023610140032

21. Avdeeva, V.V., Malinina, E.A., and Kuznetsov, N.T., *Russ. J. Inorg. Chem.*, 2017, vol. 62, no. 13, p. 1673.
https://doi.org/10.1134/S0036023617130022

22. Avdeeva, V.V., Malinina, E.A., Zhizhin, K.Yu., et al., *Russ. J. Inorg. Chem.*, 2020, vol. 65, p. 514.
https://doi.org/10.1134/S0036023620040026

23. Avdeeva, V.V., Malinina, E.A., Zhizhin, K.Yu., et al., *J. Struct. Chem.*, 2019, vol. 60, p. 692.
https://doi.org/10.1134/S0022476619050020

24. Avdeeva, V.V., Malinina, E.A., and Kuznetsov, N.T., *Russ. J. Inorg. Chem.*, 2020, vol. 65, p. 335.
https://doi.org/10.1134/S003602362003002X

25. Sivaev, I.B., *Russ. J. Inorg. Chem.*, 2019, vol. 64, p. 955.
https://doi.org/10.1134/S003602361908014X

26. Knoth, W.H., Miller, H.C., Sauer, J.C., et al., *Inorg. Chem.*, 1964, vol. 3, p. 159.

27. Johnson, J.W. and Brody, J.F., *J. Electrochem. Soc.*, 1982, vol. 129, p. 2213.

28. Preetz, W., Srebny, H.-G., and Marsmann, H.C., *Z. Naturforsch., A: Phys. Sci.*, 1984, vol. 39, p. 6.

29. Preetz, W. and Nachtigal, C., *Z. Anorg. Allg. Chem.*, 1995, vol. 621, p. 1632.

30. Scarbrough, F.E. and Lipscomb, W.N., *Inorg. Chem.*, 1972, vol. 11, p. 369.

31. Drozdova, V.V., Lisovskii, M.V., Polyakova, I.N., et al., *Russ. J. Inorg. Chem.*, 2006, vol. 51, p. 1552.
https://doi.org/10.1134/S003602360610007X

32. Drozdova, V.V., Zhizhin, K.Yu., Malinina, E.A., et al., *Russ. J. Inorg. Chem.*, 2007, vol. 52, p. 996.
https://doi.org/10.1134/S0036023607070042

33. Muetterties, E.L., Merrifield, R.E., Miller, H.C., et al., *J. Am. Chem. Soc.*, 1962, vol. 84, p. 2506.

34. Leites, L.A., *Chem. Rev.*, 1992, vol. 92, p. 279.

35. Huang, Y. and Butler, I.S., *Inorg. Chim. Acta*, 1992, vol. 192, p. 5.

36. Warneke, J., Konieczka, S.Z., Hou, G.-L., et al., *Phys. Chem. Chem. Phys.*, 2019, vol. 21, p. 5903.

37. Buslaev, Yu.A., Kravchenko, E.A., and Kolditz, L., *Coord. Chem. Rev.*, 1987, vol. 82, p. 9.

38. Kravchenko, E.A., Gippius, A.A., and Kuznetsov, N.T., *Russ. J. Inorg. Chem.*, 2020, vol. 65, p. 546.
https://doi.org/10.1134/S0036023620040105

39. Einholz, W., Vaas, K., Wieloch, C., et al., *Z. Anorg. Allg. Chem.*, 2002, vol. 628, p. 258.

40. Bowden, W., *J. Electrochem. Soc.*, 1982, vol. 129, p. 1249.

41. Kuznetsov, N.T. and Zemskova, L.A., *Zh. Neorg. Khim.*, 1982, vol. 27, p. 1320.

42. Rupich, M.W., Foos, J.S., and Brummer, S.B., *J. Electrochem. Soc.*, 1985, vol. 132, p. 119.

43. Kravchenko, E.A., Gippius, A.A., Polyakova, I.N., et al., *Z. Anorg. Allg. Chem.*, 2017, vol. 643, p. 1939.
https://doi.org/10.1002/zaac.201700293

44. Avdeeva, V.V., Polyakova, I.N., Malinina, E.A., et al., *Inorg. Chim. Acta*, 2015, vol. 428, p. 154.
https://doi.org/10.1016/j.ica.2014.12.029

45. Kravchenko, E.A., Gippius, A.A., Vologzhanina, A.V., et al., *Polyhedron*, 2016, vol. 117, p. 561.
https://doi.org/10.1016/j.poly.2016.06.016

46. Kravchenko, E.A., Gippius, A.A., Vologzhanina, A.V., et al., *Polyhedron*, 2017, vol. 138, p. 140.
https://doi.org/10.1016/j.poly.2017.09.022

47. Kravchenko, E.A., Gippius, A.A., Korlyukov, A.A., et al., *Inorg. Chim. Acta*, 2016, vol. 447, p. 22.
https://doi.org/10.1016/j.ica.2016.03.025

48. Nieuwenhuyzen, M., Seddon, K.R., Teixidor, F., et al., *Inorg. Chem.*, 2009, vol. 48, p. 889.

49. Shakirova, O.G., Daletskii, V.A, Lavrenova, L.G., et al., *Russ. J. Inorg. Chem.*, 2013, vol. 58, p. 650.

50. Avdeeva, V.V., Vologzhanina, A.V., Ugolkova, E.A., et al., *J. Solid State Chem.*, 2020, vol. 296, p. 121989.
https://doi.org/10.1016/j.jssc.2021.121989

51. Belov, A.S., Voloshin, Y.Z., Pavlov, A.A., et al., *Inorg. Chem.*, 2020, vol. 59, p. 5845.
https://doi.org/10.1021/acs.inorgchem.9b03335

52. Avdeeva, V.V., Vologzhanina, A.V., Malinina, E.A., et al., *Russ. J. Coord. Chem.*, 2019, vol. 45, no. 4, p. 295.
https://doi.org/10.1134/S1070328420050024

53. Kravchenko, E.A., Gippius, A.A., Vologzhanina, A.V., et al., *Polyhedron*, 2017, vol. 127, p. 238.
https://doi.org/10.1016/j.poly.2017.02.015

54. Avdeeva, V.V., Kravchenko, E.A., Gippius, A.A., et al., *Inorg. Chim. Acta*, 2019, vol. 487, p. 208.
https://doi.org/10.1016/j.ica.2018.12.008

55. Kleeberg, F.M. and Schleid, T., *Z. Kristallogr.*, 2017, suppl. 37, p. 107.

56. Bareiß K. and Schleid, T., *Z. Kristallogr.*, 2019, suppl. 39, p. 87.

57. Orlova, A.M., Goeva, L.V., Solntsev, K.A., and Kuznetsov, N.T., *Russ. J. Inorg. Chem.*, 1996, vol. 41, p. 769.

58. Avdeeva, V.V., Buzanov, G.A., Malinina, E.A., et al., *Crystals*, 2020, vol. 10, p. 389.
https://doi.org/10.3390/cryst10050389

59. Kuznetsov, N.T., Zemskova, L.A., and Goeva, L.V., *Koord. Khim.*, 1981, vol. 7, no. 2, p. 232.

60. Kuznetsov, N.T., Zemskova L.A., and Ippolitov, E.G, *Zh. Neorg. Khim.*, 1981, vol. 26. no. 7, p. 1862.

61. Kuznetsov, N.T. and Zemskova, L.A., *Zh. Neorg. Khim.*, 1982, vol. 27, no. 5, p. 1320.

62. Tiritiris, I. and Schleid, T., *Z. Anorg. Allg. Chem.*, 2003, vol. 629, p. 581.
https://doi.org/10.1002/zaac.200390095

63. Sivaev, I.B. and Bregadze, V.I., in *Handbook of Boron Science with Applications in Organometallics, Catalysis, Materials and Medicine*, Hosmane, N.S. and Eagling, R, Eds., World Scientific, 2019, vol. 1, p. 147.

64. Saleh, M., Powell, D.R., and Wehmschulte, R.J., *Inorg. Chem.*, 2016, vol. 55, p. 10617.
https://doi.org/10.1021/acs.inorgchem.6b01867

65. Hague, C., Patmore, N.J., Frost, C.G., et al., *Chem. Commun.*, 2001, vol. 21, p. 2286.
https://doi.org/10.1039/B106719B

66. Patmore, N.J., Ingleson, M.J., Mahon, M.F., et al., *Dalton Trans.*, 2003, vol. 14, p. 2894.
https://doi.org/10.1039/B303537A

67. Cunha-Silva, L., Carr, M.J., Kennedy, J.D., and Hardie, M.J., *Cryst. Growth Des.*, 2013, vol. 13, p. 3162.
https://doi.org/10.1021/cg4005328

68. Jenne, C. and Wegener, B., *Z. Anorg. Allg. Chem.*, 2018, vol. 644, p. 1123.
https://doi.org/10.1002/zaac.201800358

69. Tsang, C.-W., Yang, Q., and Sze, E.T.P., *et al., Inorg. Chem.*, 2000, vol. 39, p. 5851.
https://doi.org/10.1021/ic000354r

70. Anwar, S.El., Holub, J., Tok, O., et al., *J. Organomet. Chem.*, 2018, p. 89.

71. Kubasov, A.S., Turishev, E.S., Golubev, A.V., et al., *Inorg. Chim. Acta*, 2020, vol. 507, p. 119589.
https://doi.org/10.1016/j.ica.2020.119589

72. Sivaev, I.B., *Russ. J. Inorg. Chem.*, 2020, vol. 65, no. 12, p. 1854.
https://doi.org/10.1134/S0036023620120165

Translated by V. Avdeeva